QUANTUM MOLECULAR DYNAMICS STUDY OF THERMAL TRANSPORT IN SPIN JUNCTION SYSTEM

IMAM MAKHFUDZ

NATIONAL UNIVERSITY OF SINGAPORE

2008

QUANTUM MOLECULAR DYNAMICS STUDY OF THERMAL TRANSPORT IN SPIN JUNCTION SYSTEM

IMAM MAKHFUDZ

(B. Eng. (First Class Hons), NTU)

A THESIS SUBMITTED

FOR THE DEGREE OF MASTER OF SCIENCE

DEPARTMENT OF PHYSICS

NATIONAL UNIVERSITY OF SINGAPORE

2008

I certify that I have read this dissertation and that, in my opinion, in it is fully adequate in scope and quality as a dissertation for the degree of Master of Science.

_____	_____
(Wang Jian-Sheng) Principal Adviser	(Li Baowen) Co-Adviser

Approved for the University Committee on Graduate Studies

Acknowledgements

My life has always been full of dramatic turns of events and switching to pure physics after spending years of doing engineering is just another miraculous episode which though had been dreamed to happen for many years, is still a hard-to-believe reality. Doing a rather computational project but with very strong, rigorous and firm theoretical basis so that I can gain better and better understanding of theoretical physics as I go along seems to be the best way of preparing before hitting hard the innermost core of theoretical physics. This all would be impossible without the patience and parental type guidance of Prof. Wang Jian-Sheng who has in the past one and a half years nurtured my steady and exponentially increasing enthusiasm with a very mathematical physics by his utterly disciplined rigor of various aspects of statistical-solid state-many body-quantum and computational physics through his fatigueless-ness during lectures in his almost always excessively long and stomach-torturing lunch time group meetings. His discipline and strict hold onto the rule of rigor and precision even in numerical sense provides anyone a paragon for how an exact scientist is supposed to be. My sincerest thank is to him who has always ensured that I am in the right direction in my research and advised me the best suggestion one could ever give and in the most detailed way whenever I had major non-technical and especially technical difficulties. One and half years have passed with so much to learn from his lectures and classes.

I also would like to express my sincere gratitude to Prof. Li Baowen who has become my co-supervisor and given me an insightful perspective about my research. In the course of my work with Centre for Computational Science and Engineering at S10, Prof. Li has kindly permitted me to use the best computer facilities of the Centre.

The completion of my project and program would also never happen without the friendship and assistance of Prof. Wang's group members. I owe gratitude to Dr. Lü Jingtao who came to NUS at around the same time as me and who for the following one and half years so frequently let me use up his 45 minutes or more to discuss my problems and difficulties in the project. Dr. Wang Jian on the other hand has generously been my other personal mentor in writing the code as well as in computer management in our group. His only six months with me in the group has resulted in friendship which remains

warm until now.

I surely will never forget the constant companionship of the newly conferred Dr. Zeng Nan during his last nine months in NUS for his PhD program. He patiently responded to numerous emails I exchanged with him asking from the silliest to the unanswerable questions. A lot of things about being a graduate student I had discussed with him particularly how to work on computational physics. I am also indebted to Zhang Lifa who has discussed a lot with me about NEGF and given me many suggestions about my project and graduate study in general and also to Ni Xiaoxi who shared her code that used Runge-Kutta algorithm.

I will forever be indebted to Yao Donglai who has helped prove the theorem that impossible is nothing and nothing is impossible as printed on his T-shirt and also to Chen Liming et al who were really understanding in my difficult times. I also would like to thank Wu Xiang who accompanied me adapting to graduate study life in my first half year in NUS.

Last but not least I express my deep gratitude to Lim Joo Guan and Yung Shing Gene who helped me with CSE computer facilities and Teo Hwee Sim who handled my administration matters in CSE.

Table of Contents

Summary

This thesis presents the results of quantum molecular dynamics study of thermal transport in spin junction with one dimensional ferromagnetic Heisenberg model. A generalized quantum Langevin equation is derived using Green's function formalism to simulate the dynamics of the system. The simulation evaluates the time evolution of quantum mechanical operators after quasi-classical approximation rather than that of classical vectors. Holstein–Primakoff transformation is used to convert Pauli spin matrices to Bosonic operators. Quantum mechanical heat bath obeying quantum Bose-Einstein statistics is employed rather than classical heat bath. Spin wave approximation is used extensively as linear approximation to the originally nonlinear Hamiltonian. The Hamiltonian of linear spin system is expanded with respect to basis eigenstates consisting of the first excited states of ferromagnetic spin. A non-diffusive, ballistic transport is obtained from simulation and the results agree well with those obtained from other methods such as non-equilibrium Green's function (NEGF) which is exact in linear case. We have been able to not only reproduce the results which agree well with those from experiment but also obey the general rules and principles in quantum thermal transport such as the concept of ballistic and diffusive transports and the rule that the former must be the upper limit for the latter. The quantum molecular dynamics with exact and fully nonlinear force of spin-spin interaction is shown to produce non-ballistic, diffusive thermal transport. We then consider potential applications of spin thermal transport by studying possible thermal rectification effect in this spin junction by imposing asymmetry on the coupling constants between junction and leads on the two sides. Strong thermal rectification effect is observed, the variation of which with respect to degree of asymmetry in the coupling constant is investigated. Another application discussed is the use of spin junction as thermal switch. A model with controllable field in junction is proposed. We do similar analysis to derive the Langevin equation, current and noise spectrum. The simulation shows that the model has thermal switching effect as desired and this can also serve to prove the correctness of QMD formalism.

The approach that we propose here for the study of thermal transport using quantum molecular dynamics is much more general and offers greater scope of

applicability to much broader topics compared to the phenomenological theories mentioned before. There will be far less reference to material specific characteristics and more to general properties that can be stated in the language of quantum mechanics and statistical mechanics. Rather than using very speculative description of thermal transport by spin, we use very pragmatic and practical molecular dynamics simulations where the dynamics of spin system is simulated directly from the equation of motion. The non-ballistic transport at high temperatures comes about automatically and very naturally, without making debatable hypothesis as to what mechanisms have resulted in such nonlinear behavior. It is the inherent nonlinear nature of spin–spin exchange interaction force that produces the nonlinearity and the effects of which are eminent at high temperatures.

The thesis emphasizes two important aspects. First, it aims to propose theoretical (with numerical aids) explanation of experimental observations on thermal transport in spin system. With very general formulation of study of spin thermal transport, the work has been able to reproduce correctly various properties of the transport and offer semi qualitative but very consistent explanation for various phenomena observed. Secondly, the thesis would like to stress the strength of quantum molecular dynamics algorithm as proposed in [1] as the only type of molecular dynamics available thus far that is capable of simulating various quantum systems correctly [1, 2]. This new kind of molecular dynamics has very solid foundation in its conceptuality on principles of quantum and statistical mechanics. The use of quantum heat bath has overcome the inability of classical heat bath to produce correct ballistic transport at low temperatures in nonlinear case. The method also no longer uses classical variables like position coordinate and momentum that are treated classically to study systems which are inherently quantum mechanical. The use of such classical variables is not only conventional but can be conceptually wrong since quantum systems, such as spin systems, are supposed to be treated quantum mechanically and so it is not actually right to treat them classically. The proposed operator-based molecular dynamics becomes even more important because many systems like quantum spin chain cannot be represented in terms of position and linear momentum variables.

List of Figures

Chapter 1

Introduction

1.1 Introduction to Thermal Transport

The foundations of thermodynamics which provides physical explanation of macroscopic thermal phenomena had been well established by the mid of 19th century. The decades that followed saw the development of statistical mechanics in which physics community was enthusiastically searching for the microscopic and atomistic basis that underlies the principles of thermodynamics as reflected by the seminal works of Boltzmann, Gibbs, Planck, Einstein, Bose and others. The birth of quantum mechanics in 1920's rather overshadowed these excitements and possible further breakthroughs that the study of thermal physics could offer. Quantum mechanics, which prompted the birth of modern theory of solid state, dragged the attention of physics community so one-sidedly to electronic solid state physics that the other side of the industrial technology, where heat (thermal) management is daily business other than electricity, was not getting enough attention. A lot of new thermal issues become especially important in recent years when physical scale of electronic devices becomes smaller and smaller as technological sophistications are getting more and more advanced. It is well understood that energy dissipation issues dramatically increase as the system dimension drops to micro or nanoscale region. The lack of scientific attention towards thermal processes in post war era is rather surprising considering the fact that electronic and thermal transport are just the same story but with different actors. In the former the electrons play the leading role while in the latter phonons take the lead. Thermal transport may be associated more with classical thermodynamics and statistical mechanics while electronic transport with quantum theory of solids but in fact modern studies of thermal transport for example on phonons are also done based on the basic principles of quantum mechanics. In short, thermal transport essentially is on equal footing with theory of electronic transport and thus deserves as much interest from research community. With the rise of energy

efficiency problems in industry as well as in household applications that have occurred in the past few decades, study of thermal transport is steadily but certainly getting its deserved attention in scientific research as is indicated by the increase in scientific publications on this subject, investments or funding on projects and research, international collaborations as well as industrial applications and products related to thermal management.

The most basic macroscopic law governing energy transport in solid is dictated by the phenomenological equation called Fourier's law $J = -\kappa \nabla T$. The conduction process in here is characterized by thermal conductivity κ. This law applies to global non-equilibrium situations (so that energy can flow and transport happens) but very close to equilibrium state and requires local equilibrium condition in order for a temperature to be well defined [3]. Physicists have been trying to construct a microscopic theory from fundamental dynamical model that will lead naturally to this phenomenological equation in the macroscopic limit without making any statistical assumption. It is however found that Fourier's law is not valid for nanoscale systems as is normally the case when the length scale of the system (system size) becomes comparable with the length scale of the transport carrier (phonon mean free path in this case). Other than attempts to derive the equation, there has been constant debate on the finiteness of thermal conductivity in ideal models. For example, a one-dimensional atomic chain with pure harmonic interactions only will have infinite thermal conductivity and thus termed anomalous while real materials always have finite value. However, it has become better understood that nonlinear interactions of phonons from non momentum-conserving scatterings with surface and various inhomogeneities can make the conductivity finite.

Normally, thermal transport is studied microscopically using a general model consisting of two heat reservoirs connected by a junction which is whatever system we have. Each heat reservoir (also called heat bath) is kept fixed at its equilibrium temperature and it is infinitely large in size that any energy flow in or out will not change the temperature. When the temperatures of the two baths are the same, the entire system is in equilibrium and thus no heat conduction occurs. When they are different (but not so much so that the system is still very close to equilibrium), there will be temperature gradient along the junction and this is a non-equilibrium state. Transport properties such

as temperature and current are measured after steady state is achieved, that is when the system state is stationary or no longer changes with time. For phononic thermal transport, the microscopic model is normally (discrete) lattice of atoms for which local equilibrium implies that temperature can be well defined at each site according to equipartition theorem $k_B T = \left\langle p_i^2 /(2m) \right\rangle$ at the *i*-th site.

Thermal conduction is basically flow of energy which can be connected directly with the dynamics of particles which carry the thermal energy. The procedure for analysis therefore normally begins with a Hamiltonian of the microscopic system (e.g. harmonic lattice) from which one may derive the equation of motion. From the Hamiltonian of discrete lattice, one directly has the expression for local energy density and an equation of motion can be derived in straightforward manner. Generally speaking, classical treatment of thermal transport relates energy density and current according to continuity equation $\partial_t h + \partial_x j = 0$. Knowing the local energy density allows us to determine the heat flux. The interaction with heat bath at equilibrium is usually studied with molecular dynamics or Monte Carlo simulations. In non-equilibrium situations, it is only possible to do the analysis if the reservoirs are still assumed to be in equilibrium with only harmonic (linear) interactions. The degrees of freedom of heat bath can be traced out to find non-equilibrium states and derive the relevant thermodynamic quantities.

Heat baths can be classified into deterministic and stochastic types. In the deterministic heat bath, e.g. Nose–Hoover [4, 5] and iso-kinetic (Gaussian) models, the force of the heat bath on the junction is predictable and time reversible, a very convenient property. Since the junction is finite in size, it is solvable and therefore with this type of coupling to heat bath, the junction time evolution is essentially deterministic. Stochastic heat bath, on the other hand, is basically a manifestation of fluctuation-dissipation theorem in which random noise force and dissipation are introduced in the junction-heat bath coupling simultaneously. This will naturally lead to Langevin equation which summarizes the dynamics of the system. The Langevin or generalized Langevin heat bath is physically more realistic compared to deterministic heat baths. This stochastic heat bath and the associated fluctuation-dissipation theorem but with quasi-classical approximations is exactly what is used in this thesis for the quantum molecular dynamics simulations.

1.2 Introduction to Spin Thermal Transport

Spin is the building block of magnetism of solids. Materials become magnetic when there are charged particles carrying net magnetic moments such as magnetic ions. There are localized model of electronic magnetism where the spins are fixed at atom positions in the crystal and itinerant electron model of magnetism where spin carriers wander around. There are many types of interactions in a spin system including Coulomb interaction between charged spin carriers and dipole-dipole interactions between magnetic moments but the most dominant one being spin-spin super exchange interaction which is a unique type of force in spin system. Spin systems are normally modeled in terms of Hamiltonian involving only exchange interaction and external magnetic field (Zeeman term). The Hamiltonian can have one degree of freedom (called Ising model), two degrees of freedom (called XY model with its variants) or three degrees of freedom (called Heisenberg model with its variants). These models can be studied in one dimension, two dimensions or three dimensions. There is a great deal of literature resources on this subject alone which concerns us not much in this thesis. In real situations, what exist are structures with mixed or intermediate dimensionality such as spin ladder which is a quasi one-dimensional structure.

While research on magnetism initially focused on the origin of magnetism itself and recently on spin transport, giant magnetoresistance and spintronics, the study of magnetic heat transport has been increasingly receiving more attention. Thermal transport in spin systems may be not as widely studied as phonon thermal transport but it possesses its own uniqueness which makes it distinctive from phonon problem. The Hamiltonian of spin system, which is quite different from that of atomic lattice, leads to very peculiar dynamical properties and many interesting phenomena can thus be expected including those related to thermal transport.

In general, theoretical works on spin thermal transport can be classified into phenomenological theory and simulation-based. In the former work, people mostly use analogous concepts from electronic or phonon thermal transport to study the corresponding process or quantity relevant to thermal transport in magnetic system. Many authors [6, 7] use the concept of Drude weight (which originates from the theory of electronic transport) or mean free path (which is normally used in phonon thermal

transport) for spin systems [7]. Boltzmann equation [8] and linear response theory [9] have also been used to calculate thermal conductivity of spin chain materials. Other theoretical studies concern the role of spin wave such as that reported by McCollum, Wild and Callaway [10] who calculated thermal conductivity of spin wave and found roughly linear increase of thermal conductivity with temperature. These phenomenological theories use very different approaches and are frequently very much unrelated with each other. As a result, it is rather hard to make direct comparison between one and other theories. Other works which are more computationally based make use of various methods also normally used in phonon thermal transport such as Green-Kubo formalism [11, 12], master equation [12, 13] and Langevin dynamics [11, 14, 15].

On the experimental side, along with further progress in quantum theory of magnetism in 1950's, initial interests in spin thermal transport were related to that mediated by spin wave or magnon (spin wave quanta) as studied among others by Douglas [16]. Recently, similar study was done by Hess et al [17]. Several important measurements of thermal conductivity of various spin structures in real magnetic materials were performed in recent years by Sologubenko et al [18]. Research on this subject and the more general transport in one dimensional quantum systems are reviewed in reference [19]. From experimental point of view, the main challenge in the study of spin thermal transport is to separate the spin contribution from phonon contribution. This is because the spin contribution to thermal conductivity is in most situations much smaller than that of phonons. Typical curves of thermal conductivity will consist of both components. This difficulty is especially true for spin chains with isotropic exchange interaction. In quasi-one dimensional spin structures with certain degree of anisotropy, e.g. when exchange interaction in longitudinal (along the chain) direction is much larger that that in transversal direction, the separation of contributions from phonon and spin is more feasible. A unified theory of spin thermal transport that can address these issues is urgently needed and this is the direction that the work in this thesis intends to pursue.

1.3 Objective

The main objective of my research is to study thermal transport in spin chain from a different perspective, to deduce its transport properties and to design models of magnetic systems that can have possible technological applications especially as thermal control devices. We first determine the parameters that characterize thermal conductivity of spin chain. We want to use a new kind of formalism to study the dynamics of a spin junction in non-equilibrium state which is correct conceptually for studying quantum systems at all temperature regimes, general and applicable to many different transport problems as well as one which obeys basic principles of thermal transport. In the past only Monte Carlo simulation can be used to study a quantum system but only in equilibrium state. Molecular dynamics on the other hand is classical simulation and is not able to produce quantum effects. We have found a new kind of molecular dynamics which satisfies the three requirements as mentioned before. We aim to use this new formalism as an alternative approach to various theoretical and computational studies on spin thermal transport, which in our opinion, are too diverse and lacking in universality. With this novel and definitive method, we want to promote the importance of spin or magnetic systems in thermal transport to the level that their importance has been appreciated in spintronics and spin transports by highlighting what potential applications these systems may offer us. At the same time, beginning from the solid theoretical foundations that underlie our simulation, we want to contribute to enhancing theoretical understanding of physical mechanism behind thermal spin transport and we hope that this can motivate further theoretical investigations by physics community on this subject.

1.4 Organization of Thesis

The main content of the thesis starts with a preliminary part in Chapter 2 on classical spin dynamics and quantum mechanics of spin chain. Afterwards, we derive in Chapter 3 the generalized quantum Langevin equation for spin junction which constitutes the main idea of this thesis. This is to be accompanied with numerical implementation of the formalism. Simulation results on principal transport properties are presented in Chapter 4 in which we discuss both the capability of our simulation to replicate various experimental findings as well as provide physical explanation based on solid conceptual

basis that underlies the simulations. Applications of our formalism to thermal rectification phenomenon and thermal switching devices are discussed in Chapter 5. The thesis ends with a conclusion.

Chapter 2

Classical and Quantum Mechanics of Spin chain

2.1 Preliminary

This chapter contains original work presented in this thesis and is not a review of existing knowledge that is already published or known in the literature. The spin junction uses one dimensional Heisenberg model with uniform magnetic field along positive z direction. The Hamiltonian is given by

$$H = -JS^2 \sum_i \vec{\sigma}_i \bullet \vec{\sigma}_{i+1} - hS \sum_i \sigma_i^z \tag{2.1}$$

where $J > 0$ for ferromagnetic phase and $J < 0$ for anti-ferromagnetic phase.

The model structure consists of a junction in the middle part with leads on the right and on the left. The spin junction Hamiltonian can thus be symbolically written as $H = H^L + H^C + H^R + V^{LC} + V^{RC}$ where the H's represent the separate Hamiltonians for the left lead, junction and the right lead respectively while the V's represent the couplings between the junction and the leads. The leads are not interacting with each other.

2.2 Classical Spin Dynamics

In principle, spin is a quantum mechanical entity. It is supposed to be studied quantum mechanically. But we may want to simulate it classically by treating it as classical vector, that is $\vec{\sigma} = |\vec{\sigma}|\vec{e}$. The classical spin dynamics is derived as follows.

The spin equation of motion in Heisenberg model is a very fundamental dynamical equation in theory of magnetism. Because of its fundamentality, it is supposed to be derivable using elementary techniques so that who derived it first matters not much and in fact is not known or recorded in any recognized scientific journal except derivation of some variants of it (e.g. in [20]). Instead of deriving the dynamics quantum mechanically, we will demonstrate another method based on simple analogy which is most likely never discussed in literature. Being consistent with the main topic of this section, we use classical approach.

The main idea is that since spin and orbital angular momenta are both angular momentum, the former is considered "intrinsic" while the latter is "extrinsic" by quantum mechanics, they should be treated the same way and obey the same equation in classical mechanics. This is also true in quantum mechanics as suggested by, for example, the commutation relations which are the same for orbital and spin angular momenta. But here we will use Newton's second law, Lagrange equation or Hamilton's equation instead of Heisenberg or Schrödinger equation. However, it is clear that we will not be able to use any of these three equations if we stick to the conjugate coordinate and momentum variables, even in their generalized form since spin vector cannot be expressed in terms of either of these two.

We propose to derive the equation of motion for orbital angular momentum $\vec{L}$ and argue that it should apply to spin vector too. By doing so, we will be able to make use of the coordinate and momentum variables of $\vec{L}$ in the derivation using Hamilton's equation that follows. Since $\vec{L} = \vec{r} \times \vec{p}$,

$$\frac{d\vec{L}}{dt} = \frac{d\vec{r}}{dt} \times \vec{p} + \vec{r} \times \frac{d\vec{p}}{dt} \tag{2.2}$$

Using Hamilton's equations of motion $\frac{dr}{dt} = \frac{\partial H}{\partial p}, \frac{dr}{dt} = -\frac{\partial H}{\partial q}$ we obtain

$$\begin{aligned} \frac{d\vec{L}}{dt} &= \left(\frac{\partial H}{\partial \vec{p}}\right) \times \vec{p} + \vec{r} \times \left(-\frac{\partial H}{\partial \vec{r}}\right) \\ &= -\vec{p} \times \left(\frac{\partial H}{\partial \vec{p}}\right) - \vec{r} \times \left(\frac{\partial H}{\partial \vec{r}}\right) \end{aligned} \tag{2.3}$$

The analogous Hamiltonian H in terms of orbital angular momentum products can be obtained by just replacing the S by L. To simplify the derivation, we are going to omit the magnetic field part of the Hamiltonian without losing generality of the resulting equation of motion. This is justified by the fact that if the final result is valid for the dot product of two spin vectors, it should also be valid for a z component of a spin vector only because the latter can be considered to be the dot product of a spin vector and a constant spin vector pointing along z direction. Hence,

$$H = -J \sum_j \vec{L}_j \bullet \vec{L}_{j+1} = -J \sum_j \left(\vec{r}_j \times \vec{p}_j\right) \bullet \left(\vec{r}_{j+1} \times \vec{p}_{j+1}\right) \tag{2.4}$$

Using the vector product identity $(\vec{a}\times\vec{b})\bullet(\vec{c}\times\vec{d})=(\vec{a}\bullet\vec{c})(\vec{b}\bullet\vec{d})-(\vec{a}\bullet\vec{d})(\vec{b}\bullet\vec{c})$ we obtain

$$H=-J\sum_j(\vec{r}_j\times\vec{p}_j)\bullet(\vec{r}_{j+1}\times\vec{p}_{j+1})=-J\sum_j(\vec{r}_j\bullet\vec{r}_{j+1})(\vec{p}_j\bullet\vec{p}_{j+1})-(\vec{r}_j\bullet\vec{p}_{j+1})(\vec{p}_j\bullet\vec{r}_{j+1}) \tag{2.5}$$

$$\frac{\partial H}{\partial\vec{p}_i}=-J\sum_j(\vec{r}_j\bullet\vec{r}_{j+1})\vec{p}_{j+1}\delta_{ij}-(\vec{r}_j\bullet\vec{p}_{j+1})\vec{r}_{j+1}\delta_{ij}=-J\sum_j\vec{r}_j\times(\vec{p}_{j+1}\times\vec{r}_{j+1})\delta_{ij} \tag{2.6}$$

$$\frac{\partial H}{\partial\vec{r}_i}=-J\sum_j(\vec{p}_j\bullet\vec{p}_{j+1})\vec{r}_{j+1}\delta_{ij}-(\vec{p}_j\bullet\vec{r}_{j+1})\vec{p}_{j+1}\delta_{ij}=-J\sum_j\vec{p}_j\times(\vec{r}_{j+1}\times\vec{p}_{j+1})\delta_{ij} \tag{2.7}$$

where the last two lines have been obtained by making use of another vector product identity $\vec{a}\times(\vec{b}\times\vec{c})=(\vec{a}\bullet\vec{c})\vec{b}-(\vec{a}\bullet\vec{b})\vec{c}$. Substituting equations (2.6) and (2.7) into equation (2.3) we get

$$\frac{d\vec{L}_i}{dt}=-\vec{p}_i\times\left(-J\sum_j\vec{r}_j\times(\vec{p}_{j+1}\times\vec{r}_{j+1})\delta_{ij}\right)-\vec{r}_i\times\left(-J\sum_j\vec{p}_j\times(\vec{r}_{j+1}\times\vec{p}_{j+1})\delta_{ij}\right)$$

$$=-\left(-J\sum_j(\vec{p}_i\times\vec{r}_j)\times(\vec{p}_{j+1}\times\vec{r}_{j+1})\delta_{ij}\right)-\left(-J\sum_j(\vec{r}_i\times\vec{p}_j)\times(\vec{r}_{j+1}\times\vec{p}_{j+1})\delta_{ij}\right)$$

$$=J\sum_j(\vec{r}_j\times\vec{p}_i+\vec{r}_i\times\vec{p}_j)\times(\vec{r}_{j+1}\times\vec{p}_{j+1})\delta_{ij}$$

$$\frac{d\vec{L}_i}{dt}=J\sum_j(\vec{r}_j\times\vec{p}_i+\vec{r}_i\times\vec{p}_j)\times\vec{L}_{j+1}\delta_{ij} \tag{2.8}$$

Using the same vector product identity again we finally find

$$\frac{d\vec{L}_i}{dt}=J\sum_j(\vec{r}_j\times\vec{p}_i+\vec{r}_i\times\vec{p}_j)\times\vec{L}_{j+1}\delta_{ij}$$

$$=-J\sum_j\vec{L}_{j+1}\times(\vec{r}_j\times\vec{p}_i+\vec{r}_i\times\vec{p}_j)\delta_{ij}$$

$$=-J\sum_j-\delta_{ij}(\vec{r}_j\times\vec{p}_i+\vec{r}_i\times\vec{p}_j)\times\vec{L}_{j+1}$$

$$=-\vec{L}_i\times\frac{\partial}{\partial\vec{L}_i}\left(-J\sum_j\vec{L}_j\bullet\vec{L}_{j+1}\right) \tag{2.9}$$

$$=-\vec{L}_i\times\frac{\partial H}{\partial\vec{L}_i}$$

Hence, by analogy between $\vec{S}$ and $\vec{L}$,

$$\frac{d\vec{S}_i}{dt}=-\vec{S}_i\times\frac{\partial H}{\partial\vec{S}_i}\text{ or }\frac{d\vec{\sigma}_i}{dt}=-\vec{\sigma}_i\times\frac{\partial H_\sigma}{\partial\vec{\sigma}_i} \tag{2.10}$$

In equation (2.10), we define Hamiltonian $H_\sigma = -JS\sum_i \vec{\sigma}_i.\vec{\sigma}_{i+1} - h\sum_i \sigma_i^z$ to have consistent formulation. It turns out that this spin equation of motion is universal and valid for both classical and quantum cases. That is, the derivations using Hamilton equation and Heisenberg equation will give exactly the same form of equation but of course with different interpretation of spin.

Using the given Heisenberg Hamiltonian we obtain,

$$\frac{d\vec{\sigma}_i}{dt} = -\vec{\sigma}_i \times \left(-JS(\vec{\sigma}_{i-1} + \vec{\sigma}_{i+1}) - h\hat{z} \right) = \vec{\sigma}_i \times \left(JS(\vec{\sigma}_{i-1} + \vec{\sigma}_{i+1}) + h\hat{z} \right) \\ = \vec{\sigma}_i \times \vec{h}_{eff} \tag{2.11}$$

where $\vec{h}_{eff} = JS(\vec{\sigma}_{i-1} + \vec{\sigma}_{i+1}) + h\hat{z}$

Representing the classical spin vector by a column matrix with *x*, *y* and *z* components as the matrix elements, $\sigma_i = (x_i, y_i, z_i)^T$, the explicit equations of motion for the three vector components are

$$\frac{dx_i}{dt} = JS\left(y_i(z_{i-1} + z_{i+1}) - z_i(y_{i-1} + y_{i+1})\right) + y_i h,$$

$$\frac{dy_i}{dt} = JS\left(z_i(x_{i-1} + x_{i+1}) - x_i(z_{i-1} + z_{i+1})\right) - x_i h, \tag{2.12}$$

$$\frac{dz_i}{dt} = JS\left(x_i(y_{i-1} + y_{i+1}) - y_i(x_{i-1} + x_{i+1})\right),$$

subject to the constraint, due to conservation of spin angular momentum,

$$x_i^2 + y_i^2 + z_i^2 = 1. \tag{2.13}$$

where we have normalized the magnitude of spin angular momentum to unit value.

2.2.1 Spin Wave Approximation: Classical Derivation

A great simplification of equation (2.12) can be achieved if we adopt spin wave assumption where *x* and *y* components are much smaller than unity and thus the *z* component is approximately equal to one [21]. We obtain three coupled first order differential equations for three column vectors, X, Y and Z which contain respectively the *x*, *y* and *z* components of the spin vectors from all sites. These equations are

$$\frac{dX}{dt} = KY\,, \quad \frac{dY}{dt} = -KX\,, \quad \frac{dZ}{dt} = 0\,, \tag{2.14}$$

where the matrix K is given by

$$K = \begin{bmatrix} 2JS+h & -JS & 0 & 0 & 0 \\ -JS & 2JS+h & -JS & 0 & 0 \\ 0 & -JS & 2JS+h & -JS & 0 \\ 0 & 0 & -JS & 2JS+h & -JS \\ 0 & 0 & 0 & -JS & 2JS+h \end{bmatrix}. \tag{2.15}$$

This result is especially neat and we will see in the remainder of this thesis that this is a very important result which allows us to do an elegant linear study of the originally complicated nonlinear spin chain.

2.2.2 Dispersion relation of Spin Wave

From the equations of motion (2.14) we can also derive the dispersion relation. Starting from the two coupled equations,

$$\frac{dx_i}{dt} = -(2JS+h)y_i + JSy_{i-1} + JSy_{i+1}$$

$$\frac{dy_i}{dt} = (2JS+h)x_i - JSx_{i-1} - JSx_{i+1} \tag{2.16}$$

Taking the second derivative of the first equation and substituting it into the second equation we get,

$$\frac{d^2x_i}{dt^2} = -(2JS+h)\frac{dy_i}{dt} + JS\frac{dy_{i-1}}{dt} + JS\frac{dy_{i+1}}{dt}$$
$$= -(2JS+h)\left((2JS+h)x_i - JSx_{i-1} - JSx_{i+1}\right) + JS\left((2JS+h)x_{i-1} - JSx_{i-2} - JSx_i\right) + JS\left((2JS+h)x_{i+1} - JSx_i - JSx_{i+2}\right)$$
$$= -(6J^2S^2 + 4JSh + h^2)x_i + 2JS(2JS+h)x_{i-1} + 2JS(2JS+h)x_{i+1} - J^2S^2x_{i-2} - J^2S^2x_{i+2} \tag{2.17}$$

Using harmonic solution for spin wave, $x_j = x_0 e^{i(qj-\omega t)}$ and replacing the index i by j to avoid confusion with the imaginary square root of -1, we obtain

$$-\omega^2 x_0 e^{i(qj-\omega t)} \tag{2.18}$$

$$= -(6J^2S^2 + 4JSh + h^2)x_0 e^{i(qj-\omega t)} + 2JS(2JS+h)\left(e^{iq} + e^{-iq}\right)x_0 e^{i(qj-\omega t)} - J^2S^2\left(e^{i2q} + e^{-i2q}\right)x_0 e^{i(qj-\omega t)}$$

Canceling the $x_0 e^{i(qj-\omega t)}$ terms from both sides yields,

$$\omega^2 = \left(6J^2S^2 + 4JSh + h^2\right) - 4JS\left(2JS + h\right)\cos q + 2J^2S^2\cos 2q \qquad (2.19)$$

To illustrate the general shape of the dispersion relation, a plot of ω vs. q for $J = h = 0$ and $J = h = 1.0$ is given in Fig. 2.1.

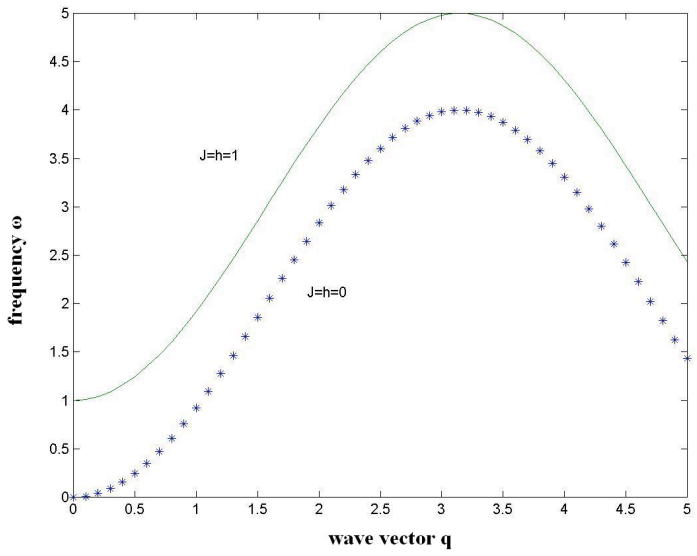

Fig. 2.1 Curves of dispersion relation of linear ferromagnetic Heisenberg spin chain with $J = 1.0, h = 0$ and $J = h = 1.0$ plotted in frequency ω as function of wave vector q. 1 unit of J is equivalent to $J = 1.4386 \times 10^{49} kg^{-1}m^{-2}$ while 1 unit of h equals $h = 17.277 KTesla$.

This dispersion relation characterizes the dependence of spin wave frequency on its wave vector. In wave scattering picture, the transport of energy in this spin chain system will then be analyzed in terms of propagation of spin wave along the spin chain and across the interfaces. Also, the dispersion relation determines the frequency bandwidth of spin wave modes which contribute to the thermal conductance of the junction.

From Fig.2.1 it can be seen that for ferromagnetic case, the spin wave dispersion relation is analogous to acoustic phonon branch. This part of the curve thus defines the first Brillouin zone of the dispersion relation with the corresponding frequency range as the bandwidth. The minimum and maximum values of frequency in first Brillouin zone for ferromagnetic case can be shown to occur at $q = 0$ and $q = \pi$ respectively with the corresponding frequency values $\omega = h$ and $\omega = 4JS + h$. Hence, the frequency bandwidth of the first Brillouin zone is always fixed to $4JS$ while the absolute value of the limiting frequencies increases or decreases by exactly the magnitude of magnetic field. In the

quasi classical molecular dynamics be discussed in later chapter of this thesis, the bandwidth will also determine the contributing frequencies of the random noise of the lead.

2.3 Quantum Mechanics of Spin Chain

2.3.1 Hilbert Space, Basis States, Eigen states

The state of an array of N spins is the tensor product of the state of each spin, written as $|\psi>=|m_1>\otimes|m_2>\otimes.....\otimes|m_N>$ (2.20)

Since each spin has $2S+1$ possible states, the Hamiltonian has $(2S+1)^N$ eigenstates and thus if we were to expand the Hamiltonian with respect to these eigenstates, the matrix would be of size $(2S+1)^N \times (2S+1)^N$. We can consider subspace of this full Hilbert space by evaluating the Hamiltonian with respect only to ground states and low lying excited states.

For the system discussed in this thesis, the Hamiltonian of spin chain can be expanded with respect to the basis states consisting of the eigenstates of the system which for a chain of N spin ½ particles, are made up of the spin up and down states for each spin [22]. For ferromagnetic Heisenberg model, spin up is parallel to magnetic field while spin down is anti-parallel to magnetic field. If we denote the former and the latter by $|0\rangle$ and $|1\rangle$ respectively, then for an array of N spins the ground state will be symbolized by $|0000....0000\rangle$, while the first and the second excited states are exemplified respectively by $|1000....0000\rangle$ and $|010.....010...0\rangle$. To be more general, a *n*-th excited state has any *n* of its *N* spins flipped down anti-parallel to magnetic field.

2.3.2 Energy Levels, Hamiltonian Matrix

In order to calculate the energy levels and Hamiltonian matrix elements of the Heisenberg model $H = -JS^2 \sum_i \vec{\sigma}_i \vec{\sigma}_{i+1} - hS \sum_i \sigma_i^z$, we rewrite it in terms of raising, lowering and *z* component Pauli spin operators σ^+, σ^- and σ^z, with the raising and lowering operators defined to be $\sigma^+ = \sigma^x + i\sigma^y$ and $\sigma^- = \sigma^x - i\sigma^y$, respectively. Their actions on the spin up and down states are

$$\sigma^+ |1\rangle = c_1 |0\rangle,\ \sigma^- |0\rangle = c_2 |1\rangle,\ \sigma^z |0\rangle = c_3 |0\rangle,\ \ \sigma^z |1\rangle = c_4 |1\rangle \tag{2.21}$$

With the constants c_1, c_2, c_3 and c_4 to be determined later from the normalization condition. (It is to be cautioned that $|1\rangle$ is a spin down ket so that it should be "raised" to get spin up ket $|0\rangle$ and vice versa). For spin ½ particles, S = ½ and we have spin up state $|0\rangle \equiv |m = 1/2\rangle = |m = S\rangle$ and $|1\rangle \equiv |m = -1/2\rangle = |m = -S\rangle$. Using standard formula in quantum mechanics for raising and lowering operators when acting on these states, noting that $S^{\pm} = S\sigma^{\pm}$,

$$\begin{aligned} S^+ |m\rangle &= \sqrt{(S+m+1)(S-m)}\,|m+1\rangle \Rightarrow \sigma^+ |m\rangle = \frac{1}{S}\sqrt{(S+m+1)(S-m)}\,|m+1\rangle \\ S^- |m\rangle &= \sqrt{(S-m+1)(S+m)}\,|m-1\rangle \Rightarrow \sigma^- |m\rangle = \frac{1}{S}\sqrt{(S-m+1)(S+m)}\,|m-1\rangle \end{aligned} \tag{2.22}$$

We obtain for S = ½,

$$\sigma^- |0\rangle = \frac{1}{S}\sqrt{(S-S+1)(S+S)}\,|1\rangle = \sqrt{\frac{2}{S}}\,|1\rangle \tag{2.23}$$

$$\sigma^+ |1\rangle = \frac{1}{S}\sqrt{(S+(-S)+1)(S-(-S))}\,|1\rangle = \sqrt{\frac{2}{S}}\,|0\rangle \tag{2.24}$$

The action of σ^z on the two one-spin eigenstates will simply take the quantum number for z component of the spin angular momentum and in summary we get the following eigenvalue equations.

$$\sigma^+ |1\rangle = \sqrt{\frac{2}{S}}\,|0\rangle,\ \sigma^- |0\rangle = \sqrt{\frac{2}{S}}\,|1\rangle,\ \ \sigma^z |0\rangle = |0\rangle,\ \ \sigma^z |1\rangle = -|1\rangle \tag{2.25}$$

The energy levels are then calculated as follows. For ground state,

$$\begin{aligned} E_0 &= \langle 000....000 | \{-JS^2 \sum_i \frac{1}{2}\left(\sigma_i^- \sigma_{i+1}^+ + \sigma_i^+ \sigma_{i+1}^-\right) + \sigma_i^z \sigma_{i+1}^z - hS\sum_i \sigma_i^z\} | 000....000\rangle \\ &= -JNS^2 - hNS. \end{aligned} \tag{2.26}$$

where it is clear that in the first sum of the Hamiltonian, only the pair products of σ^z contribute to the ground state energy.

The first excited states are found to give, in addition to the first excited energy level (that is the (diagonal) Hamiltonian matrix element between the same first excited state), due to nearest neighbor nature of the interaction, also non vanishing first off

diagonal matrix elements. Hence, the first excited state energy level (diagonal element) is,

$$\langle 00..01_i0..00 | \{-JS^2 \sum_j \frac{1}{2}\left(\sigma_j^-\sigma_{j+1}^+ + \sigma_j^+\sigma_{j+1}^-\right) + \sigma_j^z\sigma_{j+1}^z - hS\sum_j \sigma_j^z\} | 00..01_i0..00\rangle$$

$$= \langle 00..01_i0..00 | \{-JS^2 \sum_j \sigma_j^z\sigma_{j+1}^z - h\sum_j \sigma_j^z\} | 00...01_i0..00\rangle$$

$$= \langle 00...01_i0..00 | \{-J(S^2(i-2) + S^2(N-i) + S(-S) + (-S)S) - h(N-1)S - h(-S)\} | 00..01_i0..00\rangle$$

$$= -JS^2(N-2) + 2JS^2 - hNS + 2hS = -JNS^2 - hNS + 4JS^2 + 2hS$$

$$H_{ii} = E_0 + 4JS^2 + 2hS = E_0 + 2JS + h \tag{2.27}$$

The last equality follows because our derivation starts from $S = 1/2$. The importance of this last step will be clear later. In calculating (2.27), periodic boundary condition is assumed so that $|m_{N+1}\rangle = |m_1\rangle$. For off-diagonal elements, the $\sigma^+\sigma^-$ and $\sigma^-\sigma^+$ play the role and the result is

$$\langle 0..1_{i+1}...00 | \{-JS^2 \sum_j \frac{1}{2}\left(\sigma_j^-\sigma_{j+1}^+ + \sigma_j^+\sigma_{j+1}^-\right) + \sigma_j^z\sigma_{j+1}^z - hS\sum_j \sigma_j^z\} | 00....1_i..0\rangle$$

$$= \left\{-JS^2 \sum_j \frac{1}{2}\left(\langle 0..1_{i+1}...00 | \sigma_j^+\sigma_{j+1}^- | 00...1_i..0\rangle\right)\right\}$$

$$= -JS^2 \frac{1}{2}\left(\langle 0..1_{i+1}...00 | \sigma_i^+\sigma_{i+1}^- | 00...1_i..0\rangle\right)$$

$$= -JS \tag{2.28}$$

In conclusion, we have the following eigenvalue equations for the low-lying states,

$$H | 0000....0000\rangle = E_0 | 0000....0000\rangle = \left(-JNS^2 - hNS\right) | 0000....0000\rangle$$
$$H | 00...01_i0...00\rangle = E_1 | 00..01_i0...000\rangle = \left(E_0 + 2JS + h\right) | 00...01_i0...000\rangle \tag{2.29}$$
.....

so on and so forth for higher excited states. In conclusion, the system has one non-degenerate ground state and *N*-fold degenerate first excited states for array of N spins.

The complete Hamiltonian matrix evaluated with respect to all possible basis states in the full Hilbert space is graphically given in Fig.2.2.

$$
\begin{array}{ccccccccccc}
\langle 0|H|0\rangle & \langle 0|H|1\rangle & 0 & 0 & 0 & \times & \times & \times & \times & \times \\
\langle 1|H|0\rangle & \langle 1|H|1\rangle & \langle 1|H|2\rangle & 0 & 0 & \times & \times & \times & \times & \times \\
0 & \langle 2|H|1\rangle & \langle 2|H|2\rangle & \langle 2|H|3\rangle & 0 & \times & \times & \times & \times & \times \\
0 & 0 & \langle 3|H|2\rangle & \langle 3|H|3\rangle & \langle 3|H|4\rangle & \times & \times & \times & \times & \times \\
0 & 0 & 0 & \langle 4|H|3\rangle & \langle ...|H|...\rangle & \times & \times & \times & \times & \times \\
0 & 0 & 0 & 0 & \langle ...|H|...\rangle & \times & \times & \times & \times & \times \\
\times & \times & \times & \times & \times & \times & \times & \times & \times & \times \\
\times & \times & \times & \times & \times & \times & \times & \times & \times & \times \\
\times & \times & \times & \times & \times & \times & \times & \times & \times & \times \\
\times & \times & \times & \times & \times & \times & \times & \times & \times & \times
\end{array}
$$

Fig. 2.2 Matrix representation of Heisenberg Hamiltonian. The top left block represents matrix elements evaluated with respect to ground and first excited states. The elements symbolized by '×'are the one evaluated with respect to higher excited states.

The linear approximation of spin system therefore means only part of the Hamiltonian expanded with respect to the ground and first excited states are retained which is tri-diagonal. For a system of N spins in junction the Hamiltonian matrix will therefore be $N \times N$ matrix. The rest of the Hamiltonian given by higher excited states corresponds to the nonlinear part of the interaction.

The dynamics of spin system will be independent of the ground state, only dependent on the excitation energy. The excitation Hamiltonian is given by $H - E_0 I$ where I is identity matrix. Again, we obtain the same tri-diagonal matrix as that derived from classical spin dynamics (2.14). Put simply, quantum mechanically, spin wave approximation corresponds to collection of first excited states. That is, spin wave is a spin down spin propagating along the array of spins.

2.3.3 Wave Picture of Spin Wave Approximation

Another interpretation of spin wave is to regard it just as wave function where the position is discrete, localized at lattice points [22]. That is, the spin wave satisfies Schrödinger equation $i\hbar \frac{\partial \psi}{\partial t} = H\psi$ where H is the Hamiltonian matrix and ψ is a column vector with components consisting of the wave functions at individual sites (wave function as function of discrete lattice coordinate). In this linear approximation, H must

therefore be expressible as simple matrix (if the dynamics were non linear, this Schrödinger equation would remain valid, as should be the case, but the system would not most likely be solvable by this matrix formalism at all) and the matrix is exactly the tri-diagonal matrix derived before. Written element by element, the wave equation is $i\hbar\frac{\partial\psi_j}{\partial t}=\sum_i H_{ij}\psi_i$. Using harmonic solution $\psi_j = A\lambda^j e^{-i\omega t}$ with $\lambda = e^{iq}$ and the Hamiltonian matrix obtained before, we find

$$\lambda = e^{iq} = \frac{(2JS + h - \omega) \pm \sqrt{(2JS + h - \omega)^2 - 4J^2}}{2J}. \tag{2.30}$$

With little algebra it can be shown that this is just the dispersion relation (2.19) in different appearance. Hence, we find here consistency between classical and quantum mechanical interpretation of spin wave. In conclusion, spin wave is a collection of down spins propagating along the chain. Mathematically, the wave function of spin wave is linear superposition of waves of one flipped down spin at one particular site.

2.3.4 Spin Chain Hamiltonian in Second Quantization Language

We can also express spin Hamiltonian in second quantized form. In principle, in second quantization formalism, each operator is to be expressed in terms of products of two or more creation and annihilation operators which satisfy either Boson or Fermion commutation relations. To be able to do so, we have to transform Pauli spin matrices in the original Hamiltonian to creation and annihilation operators that obey either Boson or Fermion commutation relations. This is done by using Holstein–Primakoff transform introduced by Holstein and Primakoff in 1940[23].

$$\sigma^+ = \sqrt{2S}\left(1-\frac{a^\dagger a}{2S}\right)^{1/2} a, \qquad \sigma^- = \sqrt{2S}\, a^\dagger \left(1-\frac{a^\dagger a}{2S}\right)^{1/2}, \qquad \sigma^z = 1 - a^\dagger a / S, \tag{2.31}$$

$$[a_i, a_j] = [a_i^\dagger, a_j^\dagger] = 0, [a_i, a_j^\dagger] = \delta_{ij}.$$

Substituting the transformation formulas into the original Hamiltonian in terms of raising, lowering and *z* component Pauli spin operators, we obtain

$$H = -JS^2 \sum_i \frac{1}{2}\left(\sigma_i^+\sigma_{i+1}^- + \sigma_i^-\sigma_{i+1}^+\right) + \sigma_i^z\sigma_{i+1}^z - hS\sum_i \sigma_i^z \tag{2.32}$$

$$= -JS^2 \sum_i \frac{1}{2}\left(\sqrt{2/S}\left(1-\frac{a_i^\dagger a_i}{2S}\right)^{1/2} a_i \sqrt{2/S} a_{i+1}^\dagger \left(1-\frac{a_{i+1}^\dagger a_{i+1}}{2S}\right)^{1/2} + \sqrt{2/S} a_i^\dagger \left(1-\frac{a_i^\dagger a_i}{2S}\right)^{1/2} \sqrt{2/S}\left(1-\frac{a_{i+1}^\dagger a_{i+1}}{2S}\right)^{1/2} a_{i+1} \right) + \left(1-\frac{a_i^\dagger a_i}{S}\right)\left(1-\frac{a_{i+1}^\dagger a_{i+1}}{S}\right)$$

Applying the Taylor expansion and retaining only up to first order terms yields

$$\begin{aligned} &= \sum_i -\frac{JS^2}{2}\left(\frac{2}{S} a_i a_{i+1}^\dagger + \frac{2}{S} a_i^\dagger a_{i+1}\right) - JS^2 + JS^2 \frac{a_i^\dagger a_i}{S} + JS^2 \frac{a_{i+1}^\dagger a_{i+1}}{S} - hS\left(1-\frac{a_i^\dagger a_i}{S}\right) \\ &= \sum_i -\frac{JS^2}{S}\left(a_i a_{i+1}^\dagger + a_i^\dagger a_{i+1}\right) + \left(2JS^2 + hS\right)\frac{a_i^\dagger a_i}{S} - \sum_i JS^2 + hS \\ &= -JNS^2 - hNS + \sum_i -JSa_i^\dagger a_{i+1} + \left(2JS+h\right)a_i^\dagger a - JSa_i a_{i+1}^\dagger \end{aligned} \tag{2.33}$$

where by getting rid of the ground state energy term, we get

$$H = \sum_i -JSa_i^\dagger a_{i+1} + \left(2JS+h\right)a_i^\dagger a - JSa_{i+1}^\dagger a_i \equiv \sum_{ij} a_i^\dagger H_{ij} a_j \tag{2.34}$$

which in matrix form gives, again, the tri-diagonal matrix as already twice derived before.

The spin wave approximation in this representation therefore corresponds to the assumption that the creation and annihilation operators, treated as complex numbers, are much smaller than $2S$ or speaking less accurately, much smaller than unity. This is entirely consistent with classical spin dynamics interpretation where the x and y components of the spin vector are assumed to be very small compared to unity. The reason being that a and $a^\dagger$ are roughly proportional to σ^+ and σ^- respectively while these Pauli spin matrices are proportional to σ^x (x component of spin vector) and σ^y (y component of spin vector).

In summary, we have derived the same Heisenberg Hamiltonian matrix under spin wave approximation using three different and distantly related ways. It is the intention of this thesis to emphasize this spin wave approximation and its derivation for two reasons. The first reason is that the three methods of derivation each carries its own special physical meaning that is contained in the assumptions and approximations made in the derivation. The classical derivation of spin wave approximation assumes the x and y components to be much smaller than unity to put in quantitative form the classical physical picture of spin wave where the spin vectors undergo small rotation about the magnetic field (ferromagnetic ground state). The quantum mechanical derivation underlines the idea that spin wave approximation is basically equivalent to retaining only

the ground and first excited states parts of the full spin Hamiltonian. The derivation in second quantization language carries equivalent meaning as classical assumption since retaining only up to second order terms in creation and annihilation operators implies small x and y spin vector components in classical picture.

The second reason is that the spin wave approximation is linear approximation of the inherently nonlinear spin system and thus allows linear analysis of spin system. In the context of thermal transport, spin wave approximation will lead to the ballistic transport that is valid only at very low (~10 K) temperatures.

Chapter 3

Quantum Molecular Dynamics of Spin Junction

3.1 Generalized Quantum Langevin Equation

The main body of the thesis begins in this section. In the study of thermal transport in spin junction, we follow closely the modeling and formalism discussed in references [1, 24]. But there is a big difference in the sense that we are here not working with position coordinate and momentum variables, we are working with operators in second quantization language and essentially the formalism is derived quantum mechanically even though in the actual simulations the operators are merely treated as complex numbers instead of matrices and we thus actually are unable to simulate the non-commutation of non-commutating operators.

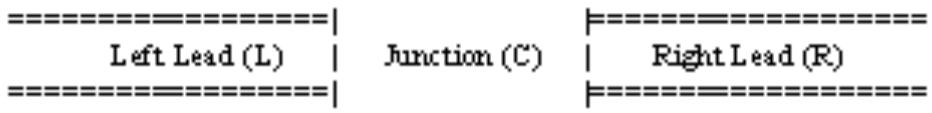

Fig.3.1 General structure of "LCR" spin junction model

Working in second quantization language, the Hamiltonian in general can be cast into the form $H = \sum_{ij} H_{ij} a_i^{\dagger} a_j$ for bosonic creation and annihilation operators $a^{\dagger}$ and a respectively. For a spin junction model with general structure shown in Fig.3.1, the Hamiltonian matrix as given in equation (2.15) can be sublet into block matrix,

$$H = \begin{bmatrix} H^L & V^{LC} & 0 \\ V^{CL} & H^C & V^{CR} \\ 0 & V^{RC} & H^R \end{bmatrix} \tag{3.1}$$

where H^L, H^C, H^R represent the left lead, junction and right lead Hamiltonians respectively while V^{LC}, V^{RC} represent the left lead–junction and right lead–junction coupling Hamiltonians respectively.

The Heisenberg equation of motion for annihilation operator $i\hbar\frac{da}{dt}=[a,H]$ can be written in terms of matrix elements as,

$$i\hbar\frac{da_i}{dt}=[a_i,\sum_{i'j'}H_{i'j'}a_{i'}^{\dagger}a_{j'}]=\sum_{i'j'}H_{i'j'}[a_i,a_{i'}^{\dagger}]a_{j'}=\sum_{i'j'}H_{i'j'}\delta_{ii'}a_{j'}=\sum_{j'}H_{ij'}a_{j'}$$

which is equivalent to, in matrix equation,

$$i\hbar\frac{da}{dt}=Ha \tag{3.2}$$

with solution (for time independent Hamiltonian) $a(t)=a(0)e^{-\frac{iHt}{\hbar}}$. Written for the column vectors of dynamical variable (annihilation operator) for the left lead, junction and the right lead, this equation gives the following three equations.

$$\begin{aligned}
i\frac{da^L}{dt}&=H^La^L+V^{LC}a^C\\
i\frac{da^C}{dt}&=H^Ca^C+V^{CL}a^L+V^{CR}a^R\\
i\frac{da^R}{dt}&=H^Ra^R+V^{RC}a^C
\end{aligned} \tag{3.3}$$

The above three equations are basically matrix equations. To solve these equations, we will use Green's function formalism. There are four Green's functions which may be used for later discussion, all of which will be associated with the lead.

$$\begin{aligned}
g^r(t,t')&=-\frac{i}{\hbar}\theta(t-t')\langle[a(t),a^{\dagger}(t')]\rangle,\quad g^a(t,t')=\frac{i}{\hbar}\theta(t'-t)\langle[a(t),a^{\dagger}(t')]\rangle\\
g^<(t,t')&=\frac{1}{i\hbar}\langle a^{\dagger}(t')a(t)\rangle,\quad g^>(t,t')=\frac{1}{i\hbar}\langle a(t)a^{\dagger}(t')\rangle
\end{aligned} \tag{3.4}$$

We will use equation of motion method where from a given homogeneous differential equation $Ly=0$, we define the corresponding equation for Green's function $Lg(t,t')=\delta(t,t')$. We then do Fourier transform to obtain the solution for Green's function in frequency domain and then do the inverse Fourier transform to obtain the corresponding solution in time domain. The homogeneous part of lead equation $i\frac{da^{\alpha}}{dt}=H^{\alpha}a^{\alpha}$ which is nothing but equation (3.2) has solution

$$a^{\alpha}(t) = e^{-iH^{\alpha}t} a^{\alpha}(0). \tag{3.5}$$

Solving the inhomogeneous equation using variation of parameters instead of Green's function method, we write $a^{\alpha}(t) = e^{-iH^{\alpha}t} f(t)$ where $f(t)$ is a time-dependent operator to be determined from the inhomogeneous equation as follows. Substituting variational solution to (3.3) we get

$$i\left(-iH^{\alpha} e^{-iH^{\alpha}t} f(t) + e^{-iH^{\alpha}t} \frac{df(t)}{dt} \right) = H^{\alpha} e^{-iH^{\alpha}t} f(t) + V^{\alpha C} a^{C}(t) \tag{3.6}$$

The $H^{\alpha} e^{-iH^{\alpha}t} f(t)$ terms on both sides cancel out to give

$$ie^{-iH^{\alpha}t} \frac{df(t)}{dt} = V^{\alpha C} a^{C}(t) \tag{3.7}$$

which is solved by

$$f(t) = f(t_0) - i\int_{t_0}^{t} e^{iH^{\alpha}t'} V^{\alpha C} a^{C}(t')dt' \tag{3.8}$$

Thus, the complete solution of $a^{\alpha}(t)$ is

$$a^{\alpha}(t) = e^{-iH^{\alpha}t} \left(f(t_0) - i\int_{t_0}^{t} e^{iH^{\alpha}t'} V^{\alpha C} a^{C}(t')dt' \right). \tag{3.9}$$

Fixing the boundary condition that $a^{\alpha}(t) = a^{\alpha}(t_0)$ at t_0, it is obvious that $f(t_0) = e^{iH^{\alpha}t_0} a^{\alpha}(t_0)$ and hence the final solution for the annihilation operator is given by,

$$a^{\alpha}(t) = e^{-iH^{\alpha}(t-t_0)} a^{\alpha}(t_0) - i\int_{t_0}^{t} e^{-iH^{\alpha}(t-t')} V^{\alpha C} a^{C}(t')dt' \tag{3.10}$$

The first term on the right hand side corresponds to free lead, not coupled to the junction. Note that this time domain expression involves H^{L} and a^{L} which we do not know since the lead is semi infinite and is therefore unsolvable for an explicit time domain expression. We only know the statistical properties of the lead in the form of distribution function we assume for the lead. Here the Green's function comes to rescue. Invoking the definition of retarded Green's function and substituting for the explicit solution for annihilation operator from (3.5), we obtain

$$g^r(t) = -\frac{i\theta(t)}{\hbar}\langle[a(t), a^\dagger(0)]\rangle = -\frac{i\theta(t)}{\hbar}\left\langle[e^{-\frac{iHt}{\hbar}}a(0), a^\dagger(0)]\right\rangle$$
$$= -\frac{i\theta(t)}{\hbar}e^{-\frac{iHt}{\hbar}} \tag{3.11}$$

We want this Green's function to follow adiabatic switch-on principle which means that at $t_o \to -\infty$, the system is completely non interacting ground state (the leads and the junction are decoupled) and the interaction is switched on slowly so that at t = 0 the system is fully interacting. This implies that the retarded Green's function be multiplied by an exponentially decay function $e^{-\eta t}, \eta > 0$ (and later take the limit $\eta \to 0$ to return to original system) so that at $t_o \to \infty$, the interaction is switched off (Note that $g^r(t)$ is nonzero only for $t > 0$). The Green's function now becomes,

$$g^r(t) = -\frac{i\theta(t)}{\hbar}e^{-\frac{iHt}{\hbar}}e^{-\eta t} = -\frac{i\theta(t)}{\hbar}e^{-\frac{i(H-i\eta)t}{\hbar}} \tag{3.12}$$

To systematically find the equation of motion satisfied by this Green's function, we take its first time derivative,

$$\frac{dg^r(t)}{dt} = -\frac{i}{\hbar}\frac{d\theta(t)}{dt}e^{-\frac{i(H-i\eta)t}{\hbar}} - \frac{i\theta(t)}{\hbar}\frac{-i(H-i\eta)}{\hbar}e^{-\frac{i(H-i\eta)t}{\hbar}}$$
$$= -\frac{i}{\hbar}\delta(t)e^{-\frac{i(H-i\eta)t}{\hbar}} - \frac{i(H-i\eta)}{\hbar}g^r(t) \tag{3.13}$$

Or in frequency domain, using the agreed convention on definition of Fourier transform, we obtain

$$-i\omega G^r[\omega] = -\frac{i}{\hbar} - \frac{i}{\hbar}G^r[\omega](H-i\eta) \tag{3.14}$$

$$((\omega + i\eta) - H)G^r[\omega] = I \quad \text{or} \quad G^r[\omega] = \frac{I}{(\omega + i\eta) - H} \tag{3.15}$$

Comparing this equation with (3.9), we see that the general solution for the lead can be written in terms of retarded Green's function as,

$$a^\alpha(t) = e^{-iH^\alpha(t-t_0)}a^\alpha(t_0) + \int_{t_0}^{t} g^{r\alpha}(t,t')V^{\alpha C}a^C(t')dt' \tag{3.16}$$

Here it is necessary to note that it is retarded surface Green's function, not the bulk one (relevant for the junction part in the study of thermal transport through junction using

NEGF formalism, here we do not need it, everything related to Green's function deals with the lead) because we are studying the lead starting from the sites near the junction all the way to infinity. That is, the "surface" refers to first few sites of the semi infinitely long lead. Also, the matrix representing the Green's function is semi infinite in size, that is, it is infinite only in one direction [the indices of the matrices are from 0 to ∞ rather than from - ∞ to ∞). Equation (3.15) is basically matrix equation between matrices that are semi infinite in size. Writing the equation explicitly in matrix form,

$$\begin{bmatrix} \omega+i\eta-(2JS+h) & JS & 0 & 0 \\ JS & \omega+i\eta-(2JS+h) & JS & 0 \\ 0 & JS & \omega+i\eta-(2JS+h) & JS \\ 0 & 0 & JS & \omega+i\eta-(2JS+h) \end{bmatrix} \begin{bmatrix} G^r_{00} & G^r_{01} & G^r_{02} & \times \\ G^r_{10} & G^r_{11} & G^r_{12} & \times \\ G^r_{20} & G^r_{21} & G^r_{22} & \times \\ \times & \times & \times & \times \end{bmatrix} = \begin{bmatrix} I & 0 & 0 & 0 \\ 0 & I & 0 & 0 \\ 0 & 0 & I & 0 \\ 0 & 0 & 0 & I \end{bmatrix} \quad (3.17)$$

The element of Green's function matrix which is necessary for further analysis is determined by the range of interaction at the boundaries. Since for spin chain the first order differential equation of motion involves only nearest neighbors, only one element of Green's function is necessary, which is G^r_{00}. By evaluating the products involving only elements of Green's function matrix in its first column, we obtain,

$$\left[\omega + i\eta - (2JS + h)\right]G^r_{00} + JSG^r_{10} = 1 \quad (3.18)$$

$$JSG^r_{l-1,0} + \left[\omega + i\eta - (2JS + h)\right]G^r_{l,0} + JSG^r_{l+1,0} = 0, \qquad l = 1,2,3,... \quad (3.19)$$

The general solution for equations of the form above is of the form,

$$G^r_{00} = -\frac{\lambda}{JS} \text{ and } G^r_{lk} = c\lambda^{|l-k|} \quad (3.20)$$

where λ is the root of equation

$$\frac{JS}{\lambda} + \left[\omega + i\eta - (2JS + h)\right] + JS\lambda = 0 \quad (3.21)$$

$$\lambda_{1,2} = \frac{-\left[\omega + i\eta - (2JS + h)\right] \pm \sqrt{\left[\omega + i\eta - (2JS + h)\right]^2 - 4J^2S^2}}{4JS} \quad (3.22)$$

chosen the one with $|\lambda| < 1$ to ensure the boundedness of the solution. The reason is that, the λ here is exactly (except little difference arising from the convergence factor η only) equal and does correspond to the λ in the wave function picture of spin wave approximation. Therefore, since $\lambda = e^{iq}$, where in general q is complex in this case, $|\lambda|$ is equal to the convergence (growth or decay) factor of the amplitude of the wave.

Therefore, to obtain bounded spin wave, since λ is complex in general, for forward propagating wave the λ must be smaller than one in absolute value so that the real part of λ will also be smaller than one. The other root $|\lambda| > 1$ represents backward propagating wave since real part of λ larger than one will make the wave decay as it propagates backward.

Substituting the general solution for the lead (3.16) into the equation for the junction part (the middle equation in equations (3.3)),

$$i\frac{da^C(t)}{dt} = H^C a^C(t) + V^{CL}\left(e^{-iH^L(t-t_0)}a^L(t_0) - i\int_{t_0}^{t} e^{-iH^L(t-t')}V^{LC}a^C(t')dt'\right) + V^{CR}\left(e^{-iH^R(t-t_0)}a^R(t_0) - i\int_{t_0}^{t} e^{-iH^R(t-t')}V^{RC}a^C(t')dt'\right)$$

$$i\frac{da^C(t)}{dt} = H^C a^C(t) + \int_{t_0}^{t} V^{CL}g_L^r(t,t')V^{LC}a^C(t')dt' + \int_{t_0}^{t} V^{CR}g_R^r(t,t')V^{RC}a^C(t')dt' + V^{CL}e^{-iH^L(t-t_0)}a^L(t_0) + V^{CR}e^{-iH^R(t-t_0)}a \quad (3.23)$$

we obtain the following Langevin-like equation which is to be referred to as the *generalized quantum Langevin equation*.

$$i\frac{da^C(t)}{dt} = H^C a^C(t) + \int_{t_0}^{t} \Sigma_L^r(t,t')a^C(t')dt' + \int_{t_0}^{t} \Sigma_R^r(t,t')a^C(t')dt' + \eta^L(t) + \eta^R(t) \quad (3.24)$$

Here, the left lead self energy $\Sigma_L^r(t,t')$ and the right lead self energy $\Sigma_R^r(t,t')$ are defined to be, respectively,

$$\Sigma_L^r(t,t') = V^{CL}g_L^r(t,t')V^{LC} \text{ and } \Sigma_R^r(t,t') = V^{CR}g_R^r(t,t')V^{RC} \quad (3.25)$$

and the last two terms are defined to be

$$\eta^L(t) = V^{CL}e^{-iH^L(t-t_0)}a^L(t_0) \text{ and } \eta^R(t) = V^{CR}e^{-iH^R(t-t_0)}a^R(t_0) \quad (3.26)$$

In analogy with Langevin equation, the second and the third terms on the right hand side of equation (3.24) can be interpreted respectively as frictional (damping) and noise forces exerted by the lead on the junction. This interpretation is quite natural since according to fluctuation–dissipation theorem, with the lead noise specified only in terms of its statistical physical properties, the lead will in one way invigorate the dynamic of the junction through the fluctuations of noise and at the same time damps the junction through the friction force. The original formalism for the phonon case is discussed in reference [1].

3.1.1 Noise Correlation Function

The noise spectrum is defined to be the Fourier transform of noise correlation function

$$\tilde{F}[\omega] = \int_{-\infty}^{\infty} e^{i\omega t} \langle \eta(t) \eta^T(0) \rangle dt \tag{3.27}$$

Substituting (3.26) with $t_0 = 0$ into (3.27),

$$\langle \eta^L(t) (\eta^L(t'))^\dagger \rangle = \langle V^{CL} e^{-iH^L t} a^L(0) (a^L(0))^\dagger e^{iH^L t'} (V^{CL})^\dagger \rangle$$
$$= V^{CL} e^{-iH^L (t-t')} \langle a^L(0) (a^L(0))^\dagger \rangle V^{LC}$$
$$= V^{CL} \langle a^L(t-t') a^{\dagger L}(0) \rangle V^{LC}$$
$$= V^{CL} \langle a^L(0) e^{iH^L (t'-t)} a^{\dagger L}(0) \rangle V^{LC}$$
$$= V^{CL} \langle a^L(0) a^{\dagger L}(t'-t) \rangle V^{LC}$$

$$\langle \eta^L(t) (\eta^L(t'))^\dagger \rangle = i\hbar V^{CL} g^>(t'-t) V^{LC} \tag{3.28}$$

$$\tilde{F}[\omega] = \int_{-\infty}^{\infty} e^{i\omega t} \langle \eta(t) \eta^T(0) \rangle dt = \int_{-\infty}^{\infty} e^{i\omega t} i\hbar V^{CL} g^>(t) V^{LC} dt$$
$$= i\hbar V^{CL} g^>(\omega) V^{LC} (1 + f(\omega))$$
$$= i\hbar V^{CL} (g^r(\omega) - g^a(\omega)) V^{LC} (1 + f(\omega))$$
$$= i\hbar (V^{CL} g^r(\omega) V^{LC} - V^{CL} g^a(\omega) V^{LC}) (1 + f(\omega))$$
$$= i\hbar (\Sigma^{rL}(\omega) - \Sigma^{aL}(\omega)) (1 + f(\omega))$$

$$\tilde{F}[\omega] = \hbar \Gamma_L(\omega) (1 + f(\omega)) \tag{3.29}$$

where $\Sigma^{r\alpha}(\omega) = V^{C\alpha} G^{r\alpha}(\omega) V^{\alpha C}$ and $\Sigma^{a\alpha}(\omega) = V^{C\alpha} G^{a\alpha}(\omega) V^{\alpha C}$ are the retarded and advanced self energies respectively of the lead in frequency domain and $f[\omega] = \left[\exp\left(\hbar\omega / k_B T \right) - 1 \right]^{-1}$. Noting the symmetry between the left and right leads, the constant term 1 in $\tilde{F}[\omega]$ can actually be replaced by any value between 0 and 1 without changing the dynamics. Therefore, the more general formula for noise spectrum is

$$\tilde{F}[\omega] = \hbar \Gamma_L(\omega) (\Delta + f(\omega)) \tag{3.30}$$

In the classical limit, $T \to \infty$ we obtain

$$\tilde{F}[\omega] = \frac{k_B T_L \hbar \Gamma[\omega]}{\omega} \tag{3.31}$$

3.1.2 Heat Current

3.1.2.1 Definition of Heat Current Based on Local Energy Density

In order to evaluate the thermal transport properties in terms of conductance, heat current has to be defined. We use two definitions of current. First definition is based on the concept of local energy density which says that the net current flowing through a site is equal to the rate of change of local energy density at that site [3]. For linear spin chain Hamiltonian,

$$H = \sum_i (2JS + h) a_i^\dagger a_i - JS a_i^\dagger a_{i+1} - JS a_i a_{i+1}^\dagger, \tag{3.32}$$

The local energy density is

$$h_i = (2JS + h) a_i^\dagger a_i - JS a_i^\dagger a_{i+1} - JS a_i a_{i+1}^\dagger. \tag{3.33}$$

The energy current or heat flux (these two terms are used interchangeably in this thesis) is defined from continuity equation, based on reference [3],

$$\frac{dh_i}{dt} = j_i - j_{i-1} \tag{3.34}$$

$$\frac{dh_i}{dt} = (2JS + h)\left(\frac{da_i^\dagger}{dt} a_i + a_i^\dagger \frac{da_i}{dt}\right) - JS\left(\frac{da_i^\dagger}{dt} a_{i+1} + a_i^\dagger \frac{da_{i+1}}{dt}\right) - JS\left(\frac{da_i}{dt} a_{i+1}^\dagger + a_i \frac{da_{i+1}^\dagger}{dt}\right).$$

Using the Heisenberg equations of motion for a_i and $a_i^\dagger$

$$i\frac{da_i}{dt} = (2JS + h) a_i - JS a_{i-1} - JS a_{i+1}, \tag{3.35}$$

$$i\frac{da_i^\dagger}{dt} = -(2JS + h) a_i^\dagger + JS a_{i-1}^\dagger + JS a_{i+1}^\dagger, \tag{3.36}$$

we obtain $\frac{dh_i}{dt} = j_{i-1} - j_i$ (3.37)

$$= i\left[JS(2JS + h)(a_i^\dagger a_{i+1} - a_{i+1}^\dagger a_i) + (JS)^2 (a_{i+2}^\dagger a_i - a_i^\dagger a_{i+2})\right]$$

$$- i\left[JS(2JS + h)(a_{i-1}^\dagger a_i - a_i^\dagger a_{i-1}) + (JS)^2 (a_{i+1}^\dagger a_{i-1} - a_{i-1}^\dagger a_{i+1})\right].$$

Hence,

$$j_i = -iJS(2JS + h)(a_i^\dagger a_{i+1} - a_{i+1}^\dagger a_i) - i(JS)^2 (a_{i+2}^\dagger a_i - a_i^\dagger a_{i+2}). \tag{3.38}$$

An important observation of this formula is that the diagonal terms are not present. They do not contribute to energy current because diagonal terms correspond to onsite potential and since current represents energy transfer between different sites, onsite potential could not have contribution. The formula also includes not only nearest neighbor, but also the next nearest neighbors' contributions since the derivation involves first time derivative of the local Hamiltonian. Also, since current is a physical quantity, it must be real. It can be shown later that the energy current as given in terms of a_i and $a_i^\dagger$ operators above is indeed real-valued. The result is valid only for linear spin chain. It is important to not that this definition is valid and exact for linear system only.

3.1.2.2 Definition of Heat Current from Lead Hamiltonian

Another definition of heat current which is more general and valid for both linear and nonlinear systems is based on the lead properties instead of those of the junction. Current is defined to be the quantum mechanical rate of change of lead energy calculated using Heisenberg equation. Using left lead Hamiltonian, this means

$$I_L = -I_R = -\left\langle \frac{dH_L}{dt} \right\rangle = -\left\langle \frac{1}{i\hbar}\left[H_L, H\right] \right\rangle . \tag{3.39}$$

Given the Hamiltonian of left lead $H_L = \sum_{jk} a_j^\dagger H_{jk} a_k$ as one block of the entire system Hamiltonian (equation (3.1)), the current is therefore,

$$\begin{aligned}
I_L &= -\left\langle \frac{1}{i\hbar}\left[\sum_{jk} a_j^{L\dagger} H_{jk}^L a_k^L , \sum_{lm} a_1^{L\dagger} V_{lm}^{LC} a_m^C + \sum_{lm} a_1^{C\dagger} V_{lm}^{CL} a_m^L \right] \right\rangle \\
&= -\left\langle \frac{1}{i\hbar} \sum_{\substack{jk \\ lm}} a_j^{L\dagger} H_{jk}^L \left[a_k^L, a_1^{L\dagger}\right] V_{lm}^{LC} a_m^C + \frac{1}{i\hbar} \sum_{\substack{lm \\ jk}} a_1^{C\dagger} V_{lm}^{CL} \left[a_m^L, a_j^{L\dagger}\right] H_{jk}^L a_k^L \right\rangle \\
&= -\left\langle \frac{1}{i\hbar} \sum_{\substack{jk \\ lm}} a_j^{L\dagger} H_{jk}^L \delta_{kl} V_{lm}^{LC} a_m^C - \frac{1}{i\hbar} \sum_{\substack{lm \\ jk}} a_1^{C\dagger} V_{lm}^{CL} \delta_{mj} H_{jk}^L a_k^L \right\rangle \\
I_L &= -\left\langle \frac{1}{i\hbar} \sum_{\substack{jk \\ m}} a_j^{L\dagger} H_{jk}^L V_{km}^{LC} a_m^C - \frac{1}{i\hbar} \sum_{\substack{lm \\ k}} a_1^{C\dagger} V_{lm}^{CL} H_{mk}^L a_k^L \right\rangle
\end{aligned} \tag{3.40}$$

which in matrix product form is equal to

$$I_L = -\frac{1}{i\hbar}\{\left\langle a^{L^\dagger} H^L V^{LC} a^C \right\rangle - \left\langle a^{C^\dagger} V^{CL} H^L a^L \right\rangle\} \tag{3.41}$$

where the term in second bracket is the Hermitian conjugate (h.c.) of the term in the first bracket. From equation (3.3),

$$\begin{aligned} V^{CL} H^L a^L &= V^{CL}\left(i\hbar \frac{da^L}{dt} - V^{LC} a^C \right) \\ &= V^{CL}\left(i\hbar \frac{d}{dt}\left(a_0^L(t) + \int_{-\infty}^{t} g^L(t,t') V^{LC} a^C(t') dt' \right) - V^{LC} a^C \right) \\ &= i\hbar \frac{d}{dt}\left(V^{CL} a_0^L(t) + \int_{-\infty}^{t} V^{CL} g^L(t,t') V^{LC} a^C(t') dt' \right) - V^{CL} V^{LC} a^C \\ &= i\hbar \dot{B}_L - V^{CL} V^{LC} a^C \end{aligned} \tag{3.42}$$

and so

$$I_L = -\frac{1}{i\hbar}\left\{ \left\langle \left(i\hbar \dot{B}_L - V^{CL} V^{LC} a^C \right)^\dagger a^C \right\rangle - \left\langle a^{C^\dagger} \left(i\hbar \dot{B}_L - V^{CL} V^{LC} a^C \right) \right\rangle \right\} \tag{3.43}$$

$$\begin{aligned} I_L &= -\frac{1}{i\hbar}\left\{ \left\langle -i\hbar \dot{B}_L^\dagger a^C - a^{C^\dagger} V^{CL} V^{LC} a^C - i\hbar a^{C^\dagger} \dot{B}_L + a^{C^\dagger} V^{CL} V^{LC} a^C \right\rangle \right\} \\ &= \left\langle a^{C^\dagger} \dot{B}_L + \dot{B}_L^\dagger a^C \right\rangle = \left\langle a^{C^\dagger} \dot{B}_L + h.c. \right\rangle = -\left\langle \dot{a}^{C^\dagger} B_L + h.c. \right\rangle \end{aligned} \tag{3.44}$$

where $B_L = \eta_L + \int_{-\infty}^{t} \Sigma(t,t') a_c(t') dt'$ is the total left lead force acting on the junction. We obtain the last line by using the fact that the expectation value of product of lead force and junction dynamical variable is constant (energy conservation) so that its time derivative vanishes. That is,

$$\frac{d}{dt}\langle AB \rangle = \left\langle \dot{A} B + A \dot{B} \right\rangle = 0 \text{, so that } \left\langle \dot{A} B \right\rangle = -\left\langle A \dot{B} \right\rangle \tag{3.45}$$

where only the parts of the block directly related to the left lead give nonvanishing commutator. The components related to the right lead, which is not directly connected to left lead, automatically give vanishing commutators. Analogous derivation using the Hamiltonian of the right lead will give the same result.

3.2 Generalized Quantum Langevin Equation: Creation Operator Version

In Section 3.1, the generalized quantum Langevin equation was formulated in terms of annihilation operator a which brought us to deal with retarded Green's function. The word "retarded" (as in other field of physics such as the term retarded potential in electrodynamics) means that anything that happens now is caused by everything that happened in the past and everything that happens now determines what will happen in future. In other words, the presence of retarded Green's function is just a manifestation of causality. The retarded self energy $\Sigma^r[\omega]$ whose time domain appears in integral kernel of friction force is one possible form of the so called spectral distribution [25]. According to reference [25], this is a positive real function which has neither poles nor zeros in the upper half-plane. It is positive in the sense that the real part is positive in the upper half-plane. That is, the spectral distribution must be analytic in there. It is our interest to study the analytical properties of the spectral distribution represented by retarded self energy $\Sigma^r(t,t')$. It turns out that the related Green's function $G^r[\omega]$ is also analytic in the upper half plane [26, 27]. Since the real part of $G^r[\omega]$ (equation (3.15)) equals the principal value of $\frac{I}{\omega - H}$ and since $\Sigma^r[\omega] = V^{CL} G^{rL}[\omega] V^{LC} + V^{CR} G^{rR}[\omega] V^{RC}$, the retarded self energy thus also satisfies the positive definite requirement of spectral distribution. In conclusion, the generalized quantum Langevin equation in terms of annihilation operator and retarded self energy is correct from mathematical point of view. As will be seen later, in terms of simulation, the use of retarded Green's function is particularly appealing because in the integration of the kernel, we will integrate forward from some time in the past to present time.

Retarded Green's function however has advanced Green's function as its counterpart of equal footing which is merely transpose conjugate of retarded Green's function ($G^a[\omega] = (G^r[\omega])^\dagger$. We suppose that if the two were equals then we have to be able to define generalized quantum Langevin equation formalism in terms of advanced Green'a function.

The derivation of generalized quantum Langevin equation in terms of creation operator and the associated advanced and "less" Green's functions follows the same path

as that in the derivation in terms of annihilation operator.

The result for each part of this version is as follows.

Generalized Quantum Langevin Equation

$$i\frac{da^{\dagger C}}{dt} = -K^C a^{\dagger C}(t) - V^{CL}\left(e^{iH^L(t-t_0)}a^{\dagger \mathrm{L}}(t_0) + \int_{t_0}^{t} g^{aL}(t'-t)V^{LC}a^{\dagger C}(t')dt'\right) - V^{CR}\left(e^{iH^R(t-t_0)}a^{\dagger \mathrm{R}}(t_0) + \int_{t_0}^{t} g^{aR}(t'-t)V^{RC}a^{\dagger C}(t')dt'\right)$$

$$= -K^C a^{\dagger C}(t) - V^{CL}\int_{t_0}^{t} g^{aL}(t'-t)V^{LC}a^{\dagger C}(t')dt' - V^{CR}\int_{t_0}^{t} g^{aR}(t'-t)V^{RC}a^{\dagger C}(t')dt' - V^{CL}e^{iH^L(t-t_0)}a^{\dagger \mathrm{L}}(t_0) - V^{CR}e^{iH^R(t-t_0)}a^{\dagger \mathrm{R}}(t_0)$$

$$i\frac{da^{\dagger C}}{dt} = -K^C a^{\dagger C}(t) - \int_{t_0}^{t}\Sigma^{aL}(t',t)a^{\dagger C}(t')dt' - \int_{t_0}^{t}\Sigma^{aR}(t',t)a^{\dagger C}(t')dt' - \eta^L(t) - \eta^R(t) \qquad (3.46)$$

Current Formula (based on local energy density)

$$j_i = iJS(2JS+h)\left(a_i^{\dagger}a_{i+1} - a_{i+1}^{\dagger}a_i\right) + i(JS)^2\left(a_{i+2}^{\dagger}a_i - a_i^{\dagger}a_{i+2}\right) \qquad (3.47)$$

Current Formula (based on lead Hamiltonian)

$$I_L = \left\langle a^{C^{\dagger}}\dot{B}_L + \dot{B}_L^{\dagger}a^C \right\rangle = \left\langle a^{C^{\dagger}}\dot{B}_L + h.c. \right\rangle = -\left\langle \dot{a}^{C^{\dagger}}B_L + h.c. \right\rangle \qquad (3.48)$$

$$B_L = -\eta^L - \int_{-\infty}^{t}\Sigma(t',t)a^{\dagger}{}_c(t')dt' \qquad (3.49)$$

Noise Frequency Spectrum

$$\left\langle \eta^L(t)\left(\eta^L(t')\right)^{\mathrm{T}}\right\rangle = i\hbar V^{LC}g^{<}(t'-t)V^{CL}$$

$$\widetilde{F}[\omega] = \int_{-\infty}^{\infty} e^{i\omega t}\left\langle \eta(t)\eta^T(0)\right\rangle dt = \hbar\Gamma_L(-\omega)f(-\omega) \qquad (3.50)$$

In the quantum Langevin equation, the most obvious difference from the annihilation operator version is that now the dynamical variable is creation operator and the sign in front of all terms are reversed. A subtle difference exists in the integration kernel where the time order is opposite to that in annihilation.

The formula for current based on local energy density does not change while that derived from lead Hamiltonian is simply redefined using the lead force and dynamical

variable in terms of creation operator. Interesting change in noise spectrum is that the greater Green's function is replaced by less than Green's function and every frequency ω term now acquires minus sign.

3.3 Generalized Langevin Equation for Nonlinear Spin Junction

For nonlinear spin junction, the Langevin equation differs from the equation (3.24) only in the first term on the right hand side where instead of product between tri-diagonal matrix *K* and a^C or $a^{\dagger C}$, we have nonlinear "force" for each site which in general cannot be expressed as product of two matrices as in linear case. We nevertheless still have to use linear spin chain for the leads, otherwise our formulation will not work. To find the explicit expressions for that nonlinear force, we start from the quantum spin equations of motion in terms of raising, lowering and z component Pauli spin operators.

$$\begin{aligned}
\frac{d\sigma_i^+}{dt} &= iJ\left[\sigma_i^z\sigma_{i-1}^+ - \sigma_i^+\sigma_{i-1}^z + \sigma_i^z\sigma_{i+1}^+ - \sigma_i^+\sigma_{i+1}^z\right] - ih\sigma_i^+ \\
\frac{d\sigma_i^-}{dt} &= -iJ\left[\sigma_{i-1}^-\sigma_i^z - \sigma_{i-1}^z\sigma_i^- + \sigma_{i+1}^-\sigma_i^z - \sigma_{i+1}^z\sigma_i^-\right] - ih\sigma_i^- \\
\frac{d\sigma_i^z}{dt} &= \frac{-iJ}{2}\left[\sigma_{i+1}^+\sigma_i^- + \sigma_i^-\sigma_{i-1}^+ - \sigma_{i+1}^-\sigma_i^+ - \sigma_i^+\sigma_{i-1}^-\right]
\end{aligned} \tag{3.51}$$

Applying Holstein-Primakoff transform gives rise to three nonlinear equations of motion in terms of two operators a and $a^\dagger$ only. In other words, there is one redundant equation. As will be discussed in more detail later, in quasi-classical approximation, we treat operators as numbers. This way, expressing a and $a^\dagger$ in terms of their real and imaginary parts, we can solve for their "forces (first time derivatives)" from any two equations. Since $a^\dagger$ is treated simply as the complex conjugate of a, that means we have three nonlinear equations for two unknown forces. This should pose no problem since the solutions of any two equations should satisfy the third equation. The resulting forces for real part *x* and imaginary part *y* turn out to be very complicated, but as will be seen later, they will give correct simulation results for nonlinear spin chain more than just qualitatively. This very pragmatic treatment is just one level of approximation. Alternative form of algorithm to solve those equations with less radical approximation may give more reliable result. In summary, from exact Heisenberg equation for Pauli spin

matrices, we end up with quasi-classical approximated solution for real and imaginary parts of annihilation or creation operators which are all that is needed to calculate transport properties of nonlinear spin chain.

3.4 Notes on Numerical Implementation

Typical molecular dynamics simulation of phonon systems evaluates the time evolution of coordinates and their conjugate momenta. Initial values of these two variables are usually generated using random number generator. That is, the generator will generate a pair of values for coordinate and momentum. With the presence of these conjugating variables, the algorithm that is used to solve the equations of motion usually relies on the interplay between these two variables. That is, the algorithm simply solves Newton's second law in terms of x and p. No other dynamical variables need to be defined in this case. Examples of such algorithms are symplectic and Verlet algorithms which rely on interplay between coordinate and momentum.

The use of conjugate variables coordinate and linear momentum is however limited to systems which involve linear translation or displacement. For systems which evolve by rotation for examples, those two variables are irrelevant and instead, angle variable and angular momentum become the quantity of interest. For motions involving orbital or non intrinsic angular momentum where dynamics is dictated by Newton's second law in angular form, angle variable may still be used in analogy with displacement. But for intrinsic spin angular momentum where we only know the angular momentum but not the rotation angle or moment of inertia (since these two are not defined for spin angular momentum), we are left only with one dynamical variable which is the spin vector itself whose x, y and z components evolve in time. Quantum mechanical analog of this is time evolution of systems characterized only by an operator, which if treated as number is complex valued in general. In such cases, the simulation will only deal with one dynamical variable (since the x, y and z components of vector or the real and imaginary parts of complex valued operator can be put into one column matrix). The form of Newton's second law of relevance here will be the one in terms of force and the dynamical variable analog of displacement itself. The problem of simulation then reduces to that similar to solving an ordinary differential equation and thus such commonly used

numerical recipe for this problem as Euler method, leap frog or Runge-Kutta algorithm can be used. The numerical problem in this case becomes more general and straightforward than the previous situation where we had to solve for coordinate and momentum simultaneously from the coupled equations form (for x and p) of Newton's second law (which are essentially Hamilton's equations).

Because of its generality, the dynamics of this form is much more suitable for quantum molecular dynamics where we more often deal with abstract operators like annihilation and creation operators with no direct and easily interpreted physical meaning. All we have to do is to derive the "force" that drives the evolution of the operator and the force itself most of the time is not the force in the sense as defined as Newton's second law. Consequently, all other quantities that follow have to be carefully interpreted since they now frequently represent some measure of a physical quantity but not necessarily the physical quantity itself with the correct unit or dimensionality or even scale or order of magnitude.

In this thesis, the dynamical quantity of interest is initially expressed in terms of spin angular momentum operators (not classical spin vectors) as defined for spin ½ spin chain in the form of Pauli spin matrices σ^x, σ^y and σ^z. Upon re-expressing them in terms of σ^+ and σ^- and performing Holstein–Primakoff transform, the dynamical variables are in terms of a and $a^\dagger$ which are Hermitian conjugate (adjoint) of each other (or simply complex conjugate of each other when treated as numbers). Only either a or $a^\dagger$ needs be evaluated and this for a chain of N spins, there are $2N$ degree of freedom corresponding to the total number of real and imaginary parts of operator a (or $a^\dagger$) at all sites). This number is exactly equal to the number of degrees of freedom if we were to evaluate the dynamics in terms of real variables (or operators) x and p since here there will be totally N variables x and N variables p for all sites.

In this work, the code is written in C language. The entire simulations deal with complex-valued operators of quantum mechanics. Since C does not have special data type for complex numbers (except perhaps the newly introduced C99), the only way to work with complex number in C is to use user-defined complex data type, that is to separate the complex number into separate real-valued real and imaginary parts. This has to be done with extreme care. The important implication of this to the dynamics of

physical system as represented by time evolution of observable operators is that the real and imaginary parts of the operator will each obey its own equation of motion. Since all numerical simulations are essentially classical physics in nature, the major consequence of trying to simulate quantum evolution is that the operators should be treated simply as numbers. To be accurate, each operator is to be represented by its expectation value. That is, e.g., operator A will be represented by its expectation value $\langle A \rangle$ which is just a (complex) number. Product of operators AB will be represented by the expectation value of the product $\langle AB \rangle$ and subsequently, to simplify algorithm, will be represented by the product of individual expectation values $\langle A \rangle \langle B \rangle$. As such, the non-commutative property of operator product cannot be simulated. In other words, AB is assumed to be the same as BA regardless of whether A and B commute or not. The Hermitian adjoint of an operator is just the complex conjugate of the number. In the simulations, the initial expectation values will be generated randomly and the simulations are repeated over a number of cycles so that effectively an operator is represented by the ensemble average of its expectation value. In this thesis, the QMD uses annihilation operator a as dynamical variable.

Chapter 4

Simulation Results and Discussions

In this chapter, we are going to present computer simulation results on basic transport characteristics and make inference about what physical mechanism underlies the phenomena displayed by those curves. One important point to note is that the parameters used in the simulations are not the actual parameters as used in experiments. They are scaled parameters used in simulations. The choice of parameters, though often not realistic, does not change the essential physics of the system.

4.1 Linear Spin Chain Simulation

Fig. 4.1 is the result of QMD simulation for spin chain with spin wave approximation as compared with NEGF result.

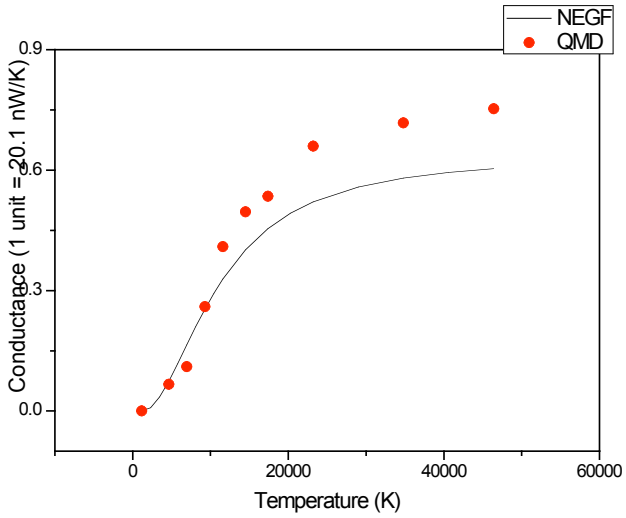

Fig. 4.1 Curve of thermal conductance σ versus temperature T for linear spin chain. Exchange interaction constant $J = 1.4386 \times 10^{49} kg^{-1}m^{-2}$ and magnetic field $h = 17.277 KTesla$. Number of spins $N = 8$ and time step is chosen to be 6.5822 × 10^{-19} s. Four cycles of 2^{22} MD steps with 10,000 steps for integration kernel of the friction force are used.

Linear spin chain yields ballistic thermal transport with conductance increasing with temperature at low temperatures and saturating at high temperatures. This ballistic transport from QMD simulations can be directly compared with NEGF [28, 29] calculation which is exact for linear case through Landauer formula [30, 31]

$$I = \int_{\omega_{\min}}^{\omega_{\max}} \frac{d\omega}{2\pi} \hbar\omega T[\omega](f_R[\omega] - f_L[\omega]), \tag{4.1}$$

where $\omega_{\max}$ and $\omega_{\min}$ are determined by the dispersion relation. From Section (2.2.2), $\omega_{\max} = h$ and $\omega_{\min} = h + 4JS$ for spin chain. Conductance is defined by

$$\begin{aligned} \sigma &= \lim_{T_R \to T_L} \frac{I}{T_R - T_L} \\ &= \int_{h}^{h+4JS} \frac{d\omega}{2\pi} \hbar\omega T[\omega] \frac{\partial f}{\partial T} \end{aligned} \tag{4.2}$$

f is Bose Einstein distribution function $f[\omega] = \left[e^{\frac{\hbar\omega}{k_B T}} - 1 \right]^{-1}$. The transmission coefficient $T[\omega]$ should be calculated using NEGF formalism, which is not discussed here, but for uniform magnetic field in all regions or no field at all in all regions $T[\omega] = 1$. Setting k_B and $\hbar$ to 1 we obtain

$$\sigma = \int_{h}^{h+4JS} \frac{d\omega}{2\pi} \omega \frac{\partial f}{\partial T} = \int_{h}^{h+4JS} \frac{d\omega}{2\pi} \frac{\omega^2}{T^2} e^{\frac{\omega}{T}} \left(e^{\frac{\omega}{T}} - 1 \right)^{-2} \tag{4.3}$$

The presence or absence of magnetic field determines the range of integration. Fig. 4.1 shows that the two methods give essentially the same result except a small numerical offset.

The pattern of the curve can be explained by considering contributions of different spin wave modes of different frequencies. Visualizing spin wave as consisting of harmonic oscillators of different frequencies where one harmonic oscillator represents one frequency mode of spin wave, at low temperatures only low frequency (energy) modes are excited and as temperature is increased, more and more higher energy (frequency) modes are excited, contributing to the transport in this low temperature regime. However, as temperature is increased further, at high temperatures, almost all

modes are excited and increasing temperature will only create slight increase in conductance that it becomes saturated. Since only linear interaction is present, this is the only effect that happens and there is no counter (e.g. nonlinear) effect that can cancel out or perhaps increase further the conductance at high temperatures. In real situation, the spin wave approximation itself is actually valid only in very low (<10 K) temperature region and the curve is therefore valid only in that part near absolute zero.

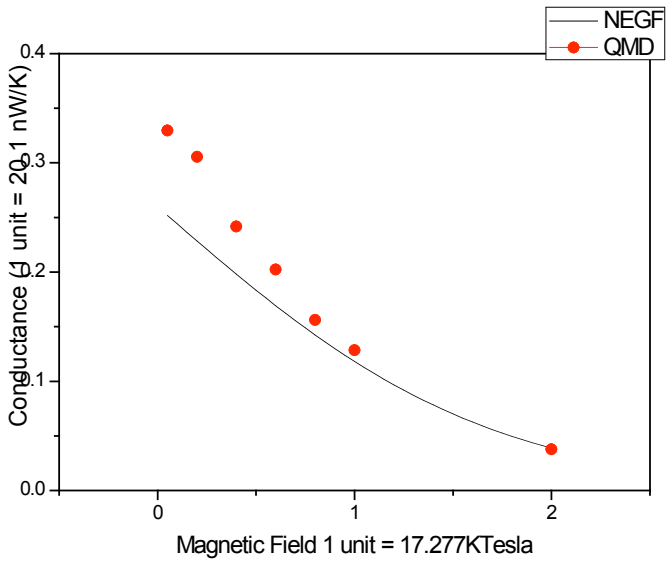

Fig. 4.2 Curve of thermal conductance σ as function of magnetic field h for linear spin chain. Exchange interaction constant $J = 1.4386 \times 10^{49} kg^{-1} m^{-2}$ and temperature $T = 5{,}800K$. Number of spins $N = 8$ and time step is chosen to be 6.5822 × 10^{-18} s. Four cycles of 2^{22} MD steps with 2,000 steps for integration kernel of the friction force are used.

Again, comparison between QMD and NEGF yields sufficiently good agreement between the two except for numerical offset which seems to be larger at smaller values of magnetic field. The behavior of conductance with magnetic field is interesting because it is peculiar to thermal transport in spin chain only. From Landauer formula, it is clear that this more or less linear drop behavior comes from the shift in the range of integration and is therefore related to the shifting up or down of the dispersion relation by the magnetic field. A similar conclusion is reached in [11].

Considering this result in terms of spin wave excitations, the magnetic field here serves to shift the energy levels of the modes as is well understood in quantum mechanics

such as the one that happens in normal Zeeman Effect. The thermal energy remains as the source of excitation energy. In the case of uniform magnetic field in z direction, it can be concluded from the Hamiltonian in second quantized form in equation (2.34) that the magnetic field contributes only to harmonic $a^{\dagger}a$ term, due to the form of Holstein–Primakoff transform for z component of spin, apart from ground state energy term. It simply adds up h to the energy of the mode $2JS$ in the absence of magnetic field which explains the linear behavior of the curve. This means in the presence of magnetic field in positive z direction, the effective mode energy is increased and thus so is the excitation energy. That means at the same temperature, there will be less modes excited and so lower thermal conductance results. It is clear that increasing the temperature will slow down the drop of the conductance and therefore higher cut off magnetic field is obtained.

4.2 Nonlinear Spin Chain Simulation

As already discussed in Section 3.3, the simulation uses the fully nonlinear spin–spin exchange interaction force. If the QMD and the conceptual basis of the thermal transport in spin chain were correct, the simulation would produce ballistic and diffusive transports in one curve with smoothly changing intermediate region between the two. This general profile of thermal conductance or conductivity is indeed what experimentalists have observed, such as that reported in references [16, 17]. However, to produce those two types of transport in one curve is one of the most challenging problems in thermal transport theory.

As to be seen later, QMD just delivers this high expectation since with the formalism developed in this thesis, ballistic transport at low temperature which changes continuously to diffusive transport at high temperature emerges so naturally with quite minimum approximation – quasi classical approximation only – and this clearly confirms the correctness of the QMD used. Other than basic assumptions, QMD evaluates spin dynamics exactly as compared to most perturbative (approximate) methods which will have to invoke major approximations or use perturbation theory. The nonlinear force considered in this simulation is not hypothetical or modeled approximately. It is physically real force that is present in any “pure” 1-D spin chain systems. In conclusion, QMD is essentially a non perturbative method.

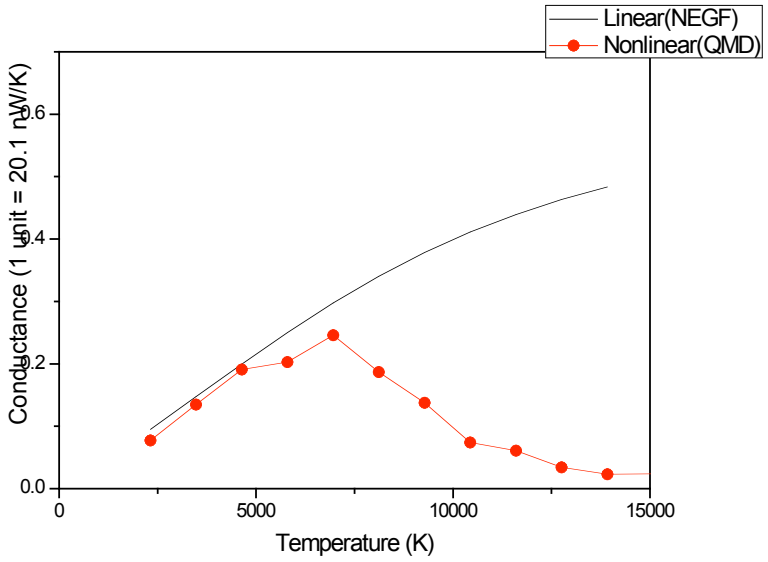

Fig. 4.3 Curve of thermal conductance σ as function of temperature T for nonlinear spin chain. Exchange interaction constant $J = 1.4386 \times 10^{49} kg^{-1} m^{-2}$ and magnetic field $h = 1.08 KTesla$. Number of spins $N = 8$ and time step is chosen to be 6.5822 × 10^{-18} s. Two cycles of 2^{20} MD steps with 2,000 steps for integration kernel of the friction force are used.

Nonlinear spin chain simulation reveals much less trivial behavior of thermal conductance with temperature and magnetic field. At low temperatures where spin wave approximation holds true, simulation must yield ballistic thermal transport in agreement with that when only linear interaction is assumed. As shown in Fig.4.3, the two curves roughly overlap with each other at low temperatures before nonlinear effects begin dominating at a transition temperature. At very high temperatures, surprisingly, the conductance does not vanish but saturates to a constant value. This phenomenon is also found in anti-ferromagnetic chain [9].

One can use the following concept to explain the high temperature behavior. We use spin wave (magnon) picture (which is actually correct only at very low temperatures) for high temperatures but we model the nonlinear interaction as inelastic scattering of spin wave quanta magnons. Thus, in this temperature regime, there will be more frequent inelastic scatterings between magnons which reduce the ballisticity of energy and

momentum transfer and so this will consequently reduce the conductance to smaller and smaller values at higher and higher temperatures. However, despite the highly diffusive transport, in the limit of very high temperature, all the modes of the spin wave are excited so as to give saturation conductance. That is, there will still be energy transported no matter how inefficient the transport is. Since ballistic thermal conductance is the largest one can get, the non linear curve should fall below the ballistic one all the time. QMD gives reasonably well behaved transitional part connecting the two regimes.

Other nonperturbative (e.g. in [11]) methods which do not use quantum heat bath mostly are only able to produce correct high temperature or low temperature behavior but fails to produce both. Since we have correct ballistic result at low temperatures, the high temperature parts of the curve from this QMD, which is more speculative, deserves more confidence than, for example, the corresponding result from method which offers correct result at high temperatures only. In the actual simulation, it is found that the transition regime always gives stronger fluctuations that longer iterations and much more carefully chosen set of simulation parameters are needed to give smoother and more reliable result. It is possible that for certain range of parameters iterations fail to converge and QMD breaks down there.

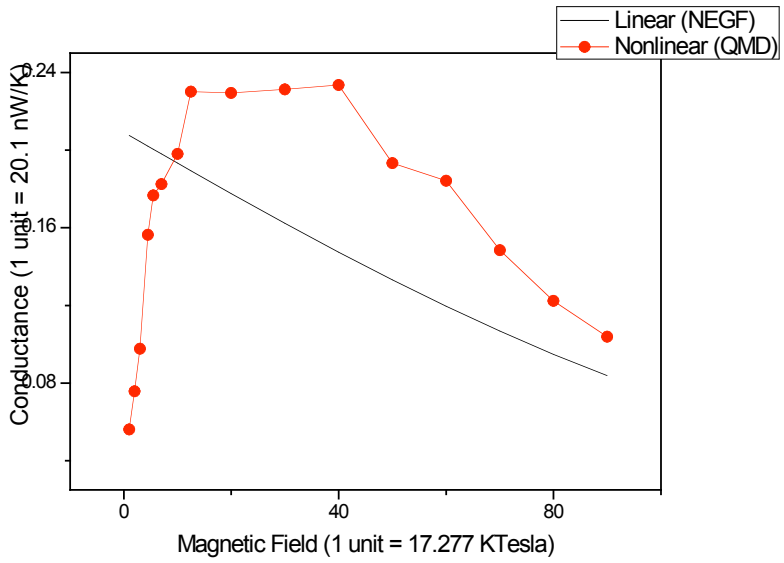

Fig. 4.4 Curve of thermal conductance σ as function of magnetic field h for nonlinear spin chain. Exchange interaction constant $J = 1.4386 \times 10^{49} kg^{-1} m^{-2}$ and temperature $T = 4{,}640K$. Number of

spins $N = 8$ and time step is chosen to be 6.5822×10^{-18} s. Two cycles of 2^{20} MD steps with 2,000 steps for integration kernel of the friction force are used.

The QMD result for conductance vs. magnetic field is even more intriguing. There is very radical change at low magnetic field region where instead of dropping with the field, the conductance increases with the field.

One can explain the peculiar behavior in low magnetic field regime by realizing that in nonlinear spin chain there are several competing influences. First competition is between linear and nonlinear parts of interaction while another one concerns the effect of magnetic field. On one hand, as mentioned before, magnetic field increases the energy levels of the modes and their excitation energies that higher magnetic field means fewer excited modes and field increase thus leads to conductance decrease. On the other hand, as can be observed from the Hamiltonian, magnetic field contributes only to the linear part of the interaction and thus field increase gives rise to more ballistic transport.

What happens at low magnetic field regime is that the widening of energy level spacing is not significant enough because the magnetic field is too weak. In spin chain with no linear assumption, the thermal energy makes the spins move freely around far away from the ground state and these result in very low conductance. But once the field is applied however weak it is, it will pull the spins together forcing them to stay close to the ground state. Stronger magnetic field means spin wave approximation becomes more valid as the spins will be held tighter to the ground state configuration. Consequently, in this weak field regime, increasing magnetic field will increase the conductance. The absence of such low magnetic field behavior in linear case is simply because with no nonlinearity, the conductance is already at the peak when no field is present. Once the field is applied, instead of pulling the spins closer to the ground state (the spins are already near ground state), the field raises the spin wave excitation energy and thus hinders more magnons from participating in the transport. The conductance thus drops from the start.

In the strong magnetic field limit, the nonlinear force is virtually completely suppressed that the widening of energy level spacing dominates. Therefore, even though energy and momentum transfer through magnon scatterings may be more elastic and

efficient, there are just much fewer magnon modes excited due to the "expensive" excitation energy and thus the conductance drops. In the limit of very strong magnetic field, the increase in excitation energy effect, which is the dominant influence in the ballistic case, becomes so dominant that the ballistic and nonlinear curves converge to the same curve. It is important not to confuse the physical explanation of conductance vs. magnetic field curve with that of conductance vs. temperature curve. Under very strong magnetic field, the nonlinear transport becomes more and more ballistic while at very high temperature, the nonlinear transport becomes less and less ballistic (more ballistic at low temperatures). Comparing the linear and nonlinear spin chains, the conductance vs. temperature curves overlap at low temperatures, while the conductance vs. magnetic field curves overlap at high magnetic field limit.

Normally, the ballistic-diffusive classification of thermal transport is defined on conductance vs. temperature curve but in spin chain system there can be question whether we can regard the low field regime in nonlinear spin chain as diffusive regime and strong field regime as ballistic regime. Fig. 4.4 gives QMD result performed at $T = 4{,}640\ K$ which is legitimately ballistic based on the hypothetical (not actual ones from real experiment) parameters chosen for the simulation. It turns out that, another simulation performed at $T = 11{,}600\ K$ which is diffusive, also shows similar low field behavior. In other words, the behavior cannot be firmly associated with diffusivity. It does arise from nonlinearity but it can not be regarded as a characteristic of diffusive transport as evidenced by those simulations results

In the study of thermal transport in spin system, the concept of nonlinearity seems to potentially cause misinterpretation or even contradiction. There should be distinction between the concept of nonlinear interaction in the sense of nonlinear spin–spin exchange interaction which is more effective at low temperatures with the concept of nonlinearity in the sense of momentum non-conserving inelastic scatterings (of spin waves or magnons) which is more effective at high temperatures. Nonlinearity is said to play more important role at low temperatures in reference [11]. The common understanding in phonon thermal transport is that nonlinearity is more significant at high temperatures [3]. With the distinction between the two contexts of nonlinearity, the two situations should not be interpreted as paradox.

In the context of spin system, at low temperatures the nonlinear spin–spin exchange interaction is very dominant because thermal kinetic energy is too low to be able to disfigure the spin assembly. The exchange interaction contains both linear (carried by *z* component of spin vector) as well as nonlinear (carried by *x* and *y* components of spin vector). Thus, nonlinearity in the sense of exchange interaction contributes to both ballistic and diffusive transports. At high temperatures, thermal kinetic energy severely disorientates spins configuration and this can be represented in wave picture as inelastic scattering between spin waves. That is, nonlinearity in the sense of inelastic scattering between spin waves contributes to diffusive transport only.

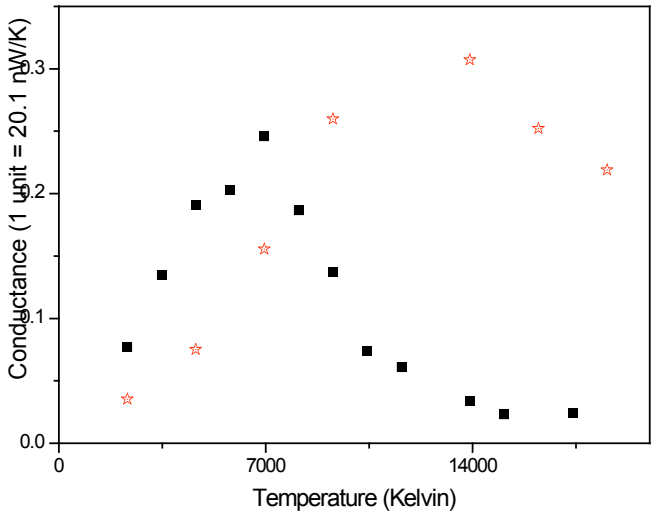

Fig. 4.5 Curves of thermal conductance σ as function of temperature T for two nonlinear spin chains with exchange interaction constants $J = 1.4386 \times 10^{49} kg^{-1}m^{-2}$ (squares) and $J = 7.193 \times 10^{49} kg^{-1}m^{-2}$ (stars) respectively but with magnetic field $h = 1.08 KTesla$ for both. Number of spins $N = 8$ and time step is chosen to be 6.5822 × 10^{-18} s. Two cycles of 2^{20} MD steps with 2,000 steps for integration kernel of the friction force are used.

Depicted on Fig. 4.5 are two spin chains having different exchange interaction constant. This figure is perfectly consistent with saturation *σ vs. J* in ballistic case, both from QMD and exact NEGF calculation using Landauer formula which shows that the maximum conductance is proportional to exchange interaction constant *J*. To be precise, the *J* dependence of maximum conductance in ballistic can be calculated as follows.

Saturation of conductance occurs at very high temperature, so using Landauer formula and taking the high temperature limit we can make approximation $e^{\frac{\omega}{T}} \approx 1 + \frac{\omega}{T}$ to come up with,

$$\sigma = \int_{h}^{h+4JS} \frac{d\omega}{2\pi} \omega \frac{\partial f}{\partial T} = \int_{h}^{h+4JS} \frac{d\omega}{2\pi} \frac{\omega^2}{T^2} e^{\frac{\omega}{T}} \left(e^{\frac{\omega}{T}} - 1 \right)^{-2}$$
$$\approx \int_{h}^{h+4JS} \frac{d\omega}{2\pi} \frac{\omega^2}{T^2} \left(1 + \frac{\omega}{T} \right) \left(1 + \frac{\omega}{T} - 1 \right)^{-2} \approx \frac{2JS}{\pi} \tag{4.4}$$

It can be concluded that the magnitude of saturation conductance in ballistic transport of spin system is largely determined by the strength of spin–spin exchange interaction coupling constant *J*. So, if we fix value of *J*, no matter what magnetic field we apply, as long as spin wave approximation is valid, the magnitude of conductance saturation will remain the same.

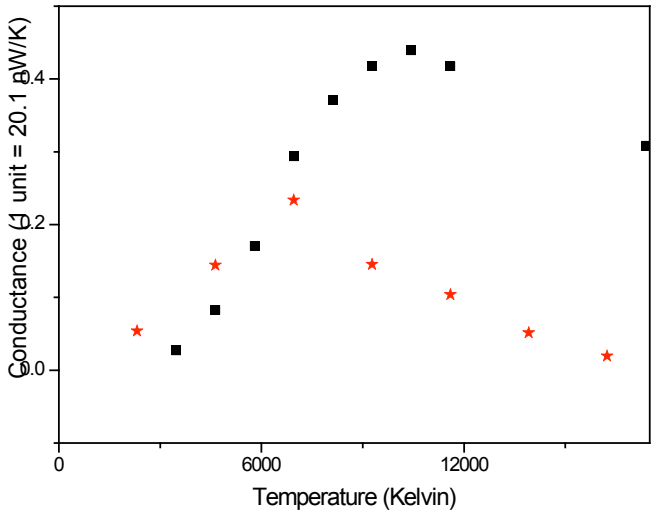

Fig. 4.6 Curves of thermal conductance σ as function of temperature T for two nonlinear spin chains with magnetic field $h = 1.73 KTesla$ (squares) and $h = 1.38 KTesla$ (stars) respectively but with exchange interaction constant $J = 1.4386 \times 10^{49} kg^{-1} m^{-2}$ for both. Number of spins $N = 8$ and time step is chosen to be 6.5822 × 10^{-18} s. Two cycles of 2^{20} MD steps with 2,000 steps for integration kernel of the

friction force are used.

Fig. 4.6 shows two curves of conductance vs. temperature for spin chains with the same coupling constant but subjected to different magnetic fields. The one with stronger magnetic field gives larger slope at low temperatures and larger conductance at high temperatures. This clearly confirms preposition that magnetic field contributes only to ballistic part of the transport. A closer look at the two curves on Fig. 4.6 shows that in ballistic low temperature regime higher magnetic field results in lower conductance while in the high temperature part higher magnetic field gives larger conductance. This is consistent with the idea that ballistic transport is strengthened by stronger magnetic field, resulting in conductance decreasing with field in ballistic regime and vice versa in region where ballisticity is overcome by nonlinearity. That is, Fig. 4.4 and Fig. 4.6 essentially contain the same physical idea.

4.3 Diffusivity of Thermal Transport in Nonlinear Spin Chain

Ballistic and diffusive are two very basic and universal modes of thermal transport. Ballistic transport is normally associated with linear system where the Hamiltonian consists of only 0-th and second order products of operators. In phonon case, this would mean constant terms or square of momentum (corresponding to kinetic energy) or square of a displacement or product of two displacements at two different sites (related to the potential energy of the system). 0-th order or constant terms will as usual be omissible since it will vanish under differentiation and thus not affect the dynamics. The quadratic terms (which can be obtained by taking the Taylor series expansion of the potential energy function of any (analytic, nonsingular) form with respect to coordinate around equilibrium position so that the first order term vanishes) are the standard constituents of harmonic oscillator Hamiltonian and are therefore called harmonic. In terms of force, such terms are associated with linear spring-like force of harmonic oscillator $\vec{F} = -k\vec{x}$ where k is the spring constant $k = \left(\frac{\partial^2 V}{\partial x^2} \right)_{x_0}$. With respect to the Hamiltonian, any displacement terms with power other than zero or two (1, 3, 4, 5, 6, etc.) will not produce such linear force and are therefore called anharmonic (unless a

transformation is performed that converts the original variables to new ones in such a way that the new Hamiltonian will involve quadratic harmonic products). Harmonic (harmonic-oscillator like) Hamiltonians are integrable and exactly solvable and are associated with momentum and energy conserving interactions. In some sense, in this system, there is no energy leakage or wasted as dissipation. In the context of thermal transport, momentum conserving situation is the most ideal situation that one can have, that is, the transport efficiency is at maximum in this situation. From the perspective of non-equilibrium statistical physics, the particles that act as the carriers of the heat energy propagate with $x \sim t$. Unfortunately, according to Fourier's law,

$$J = -\kappa \nabla T = -\kappa \frac{\Delta T}{L} = -\left(\frac{\kappa}{L}\right)\Delta T = -\sigma(\Delta T), \tag{4.5}$$

the thermal conductivity κ is proportional to system size L because the thermal conductance σ is constant with respect to L. Hence, purely harmonic Hamiltonian will result in divergent, infinite thermal conductivity in thermodynamic limit $(L, N \to \infty)$ and this is not correct physically. But that is what we will obtain if we study thermal transport by merely using harmonic Hamiltonian without including any nonlinear, anharmonic terms. A harmonic system is the most perfect system but of course real system can never be purely harmonic. Any physically real thermal conductivity should be finite.

Anything that is not linear or harmonic will produce something not ballistic. The other basic mode of transport is diffusive mode but the definition of diffusive is much more precise than just the presence of anharmonic or nonlinear interactions. To be more specific, according to Fourier's law, in diffusive transport the thermal conductance σ is inversely proportional to system size L $(\sigma \propto L^{-1})$ because thermal conductivity κ is constant with respect to L. In fact, with the precise definition to be discussed right following this paragraph, the presence of a nonlinear anharmonic interaction does not necessarily imply diffusivity because it may happen that diffusivity definition is not satisfied despite the presence of the former. In other words, there is possibility that the thermal transport is neither ballistic nor diffusive.

People normally study time correlation function to determine diffusivity or ballisticity of a transport in a model. In the context of one-dimensional spin chain, in the presence of magnetic field, no conclusive answer is confirmed whether the transport is

indeed diffusive though it is believed to be so. Our simulations also could not get convincing evidence that one-dimensional Heisenberg model, as simulated by nonlinear spin chain, is diffusive as we suppose. After all, the seemingly diffusive behavior of spin thermal transport at high temperatures does not really satisfy the precise definition of diffusivity in terms of size dependence of thermal conductance or conductivity.

Chapter 5

Applications

5. 1 Heat Rectification in Nonlinear Spin Junction

Different from rectification in electronic transport, rectification in thermal transport is relatively new concept and has received serious attention only in recent years, starting from the work reported in reference [32]. Thermal rectification is widely studied by Li et al [33] who have systematically studied this effect by numerical simulations and proposed models of thermal diode and transistor as the potential applications. Thermal rectification phenomenon itself has been observed experimentally. It has been understood (see e.g. [34]) that heat rectification in nanoscale devices requires nonlinearity and asymmetry as the two conditions for it to take effect. The nonlinearity is embodied in spin system while asymmetry can physically be introduced by imposing different exchange interactions (e.g. choosing different atoms or chemical bonds at the junction–heat bath interfaces). The degree of asymmetry here is represented by parameter χ and the coupling constants at the two junctions are

$$V_{lc} = J(1+\chi) \qquad V_{rc} = J(1-\chi) \tag{5.1}$$

It is important to remember that the energy is transported from spin to spin through the kinetic motion of the spins which interact with their nearest neighbors. Therefore, it is easy to predict that the current flowing from higher to lower temperature leads will be larger when the higher temperature side is more weakly coupled than lower temperature side because the former has enough thermal energy to “shake” the spins to transport it and thus does not need too strong coupling to be able to transfer its energy to the junction while the latter has to have strong coupling to compensate for its thermal energy which is too low to “shake” the spins to support the energy flow. Imposing stronger coupling to the hotter lead makes the junction less effective.

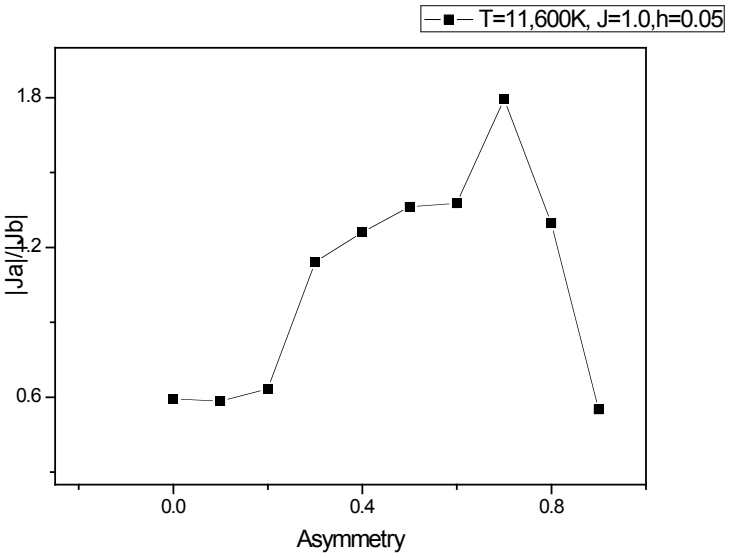

Fig.5.1 Heat rectification as measured by the ratio of the absolute values of currents in the two situations as function of degree of asymmetry χ. Parameters used are $J = 1.4386 \times 10^{49} kg^{-1}m^{-2}$, $h = 0.86385 KTesla$ and $T = 11{,}600K$. Number of spins $N = 8$ and time step 6.5822 × 10^{-18} s. Two cycles of 2^{22} MD steps with 2,000 steps for integration kernel are used.

In Fig. 5.1, the rectification strength is measured by simply comparing the magnitude of the currents in the two situations where *Ja* denotes the current flowing when hotter lead has weaker coupling while *Jb* represents that when hotter lead has stronger coupling. The simulation shows unusually high rectification in spin junction and so this is good news, probably because the system is excessively nonlinear due to cross product in equation of motion. This system thus offers much superior performance than other systems such as phonon junction as studied by Li [33] et al and two–level system (TLS) as investigated by Segal et al [34]. It is commonly understood that in most situations, spin contribution to thermal transport is too small compared to that of phonon. However, with this terrific rectification property, spin systems make a good candidate to be used in thermal rectification (e.g. diode, transistor) devices.

In his PhD thesis [35], Z. Nan argues that spectrum mismatch (in addition to nonlinearity) between left and right leads is the cause of heat rectification in atomic junction with mass gradient [36]. In some sense, the spectrum mismatch is just another form of asymmetry. By the same argument, in a spin junction, heat rectification should

also occur if the magnetic field in the two leads were different since dispersion relation shifts linearly with magnetic field. This is one other possible realization of spin thermal control.

5.2 Magnetic Thermal Switch

The properties of thermal transport in spin chain in terms of conductance variation with temperature and magnetic field have been studied in Chapter 4. It may be suggested that we construct a thermal switching device by changing temperature or tuning the magnitude of magnetic field. While this is certainly feasible, we may want to look at other factor which may serve better way of controlling the transport. Instead of changing the magnitude of magnetic field, the more mechanical and thus more commonly used control mechanism is to change the direction of magnetic field. The junction system needs to be designed in certain way that the current peaks when the magnetic field is oriented in certain direction and decreases with the increase in deviation from that orientation.

One possible model is to apply uniform magnetic field along certain direction in the leads and vary the field direction in the junction. Intuitively, when the field in the junction is parallel to those in the leads, the current flowing will be maximum and it decreases with deviation angle. QMD can be used to study this model in order to verify the correctness of the QMD itself (as compared to intuition) as well as to find possible interesting effects. It will be seen later that the Hamiltonian of the system involves anharmonic terms (odd product of creation or annihilation operator) due to the presence of magnetic field in x and y directions even if spin wave approximation has been used. Fortunately, with its simple but effective approach, QMD can handle any kind of nonlinear Hamiltonian terms which may be tough if not impossible for any other method to handle. In the following analysis, linear spin chain is assumed and therefore the rotation angle cannot be very large for the simulation result to be valid. In order for the spin wave assumption to be as valid as possible, the temperature should be relatively low with respect to system's temperature scale. The ground state about which the spin wave propagates is indeed different between the lead and the junction. That is, the spin wave has different polarization in the lead and the junction and thus undergoes polarization

rotation ("twist") at the junction-lead interface. Because the ground states in the two regions are different, we have to define separate coordinate systems for the regions and perform transformation between them so that the analysis can be done within one coordinate system, either in the coordinate system of the lead or the junction.

5.2.1 Model Structure and Analysis

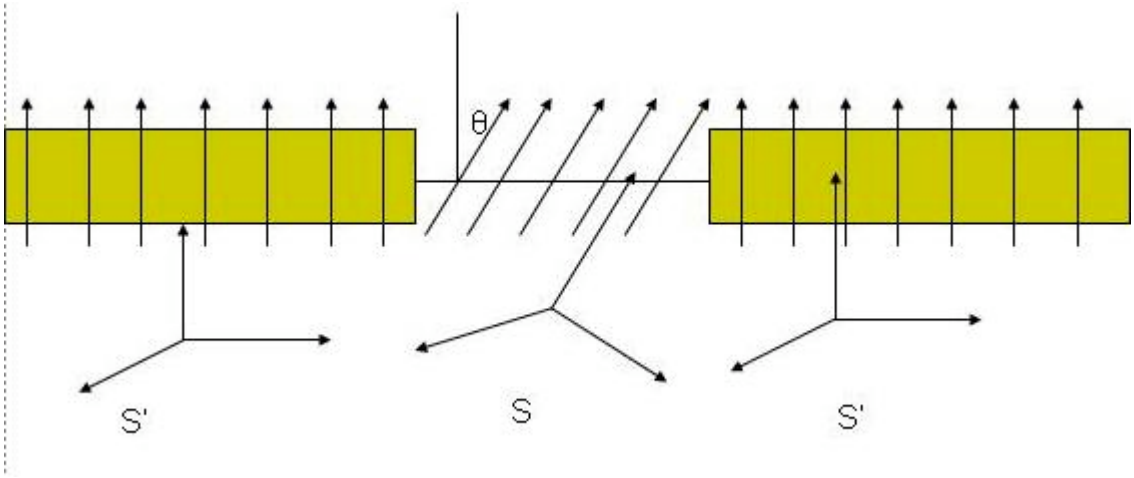

Fig. 5.2 Structure of the magnetic thermal switch. Magnetic field in the lead is fixed to point along positive *z* axis while that in the junction is oriented along arbitrary direction.

We define coordinate system *S* for central region where the *z* axis is along direction of magnetic field and *S′* is for the leads with *z* axis is vertically upward, parallel to the magnetic field there. From this point onwards, any variable without prime is associated with *S* and those with prime are associated with *S′*. The ground state of the system is such that the energy is minimized and assuming strong magnetic field, so that the spins at the sites near lead-central borders are aligned parallel to the field in the respective region instead being parallel to the neighboring spin in the neighboring region, the ground state configuration will be just that spins are parallel to magnetic field in the corresponding region. The Hamiltonian of central region will be (in *S* coordinate system)

$$H^c = -J\sum_{ij}\bar{\sigma}_i.\bar{\sigma}_j - \sum_i h\sigma_i^z \tag{5.2}$$

where $\vec{h}\bullet\vec{\sigma}_i$ automatically gives the $h\sigma_i^z$ because the spin is parallel to the magnetic

field along z axis of S.

We define rotation transformation R from S to S' acting on spin vector operator in S specified by polar angle θ and azimuthal angle ϕ of magnetic field of central region with respect to S', so that the z axis of S are rotated to be parallel to the z' axis of S'.

$$\bar{\sigma}' = R\bar{\sigma} \text{ or } \bar{\sigma} = R^{-1}\bar{\sigma}' \tag{5.3}$$

Explicitly, the rotation transformation matrix R is given by

$$R = \begin{bmatrix} \cos\theta_{hs}\cos\phi_{hs} & -\sin\phi_{hs} & \sin\theta_{hs}\cos\phi_{hs} \\ \sin\phi_{hs}\cos\theta_{hs} & \cos\phi_{hs} & \sin\theta_{hs}\sin\phi_{hs} \\ -\sin\theta_{hs} & 0 & \cos\theta_{hs} \end{bmatrix} \tag{5.4.a}$$

or

$$R^{-1} = \begin{bmatrix} \cos\theta_{hs}\cos\phi_{hs} & \sin\phi_{hs}\cos\theta_{hs} & -\sin\theta_{hs} \\ -\sin\phi_{hs} & \cos\phi_{hs} & 0 \\ \sin\theta_{hs}\cos\phi_{hs} & \sin\theta_{hs}\sin\phi_{hs} & \cos\theta_{hs} \end{bmatrix} \tag{5.4.b}$$

Hence, we can re-express the Hamiltonian in terms of σ' and refer to the resulting Hamiltonian as H^{c}',

$$H^{c}' = -J\sum_{ij} R^{-1}\bar{\sigma}_i'.R^{-1}\bar{\sigma}_j' - \sum_i hR^{-1}\sigma_i^{z}' \tag{5.5}$$

Since a dot product between two vectors (operators) depends only on the angle between them, it is rotational invariance. That is, without evaluating explicitly the first sum, it is clear that $R^{-1}\bar{\sigma}_i.R^{-1}\bar{\sigma}_j = \bar{\sigma}_i'.\bar{\sigma}_j'$ while the second term, originally in S involves only the z component of magnetic field, can now be rewritten in more general form as

$$hR^{-1}\bar{\sigma}_i^{z}' = \left(h\begin{bmatrix} R_{11}^{-1} & R_{12}^{-1} & R_{13}^{-1} \\ R_{21}^{-1} & R_{22}^{-1} & R_{23}^{-1} \\ R_{31}^{-1} & R_{32}^{-1} & R_{33}^{-1} \end{bmatrix}\begin{bmatrix} \sigma_i^{x}' \\ \sigma_i^{y}' \\ \sigma_i^{z}' \end{bmatrix}\right)^{z} = \left(h\begin{bmatrix} R_{11}^{-1}\sigma_i^{x}' + R_{12}^{-1}\sigma_i^{y}' + R_{13}^{-1}\sigma_i^{z}' \\ R_{21}^{-1}\sigma_i^{x}' + R_{22}^{-1}\sigma_i^{y}' + R_{23}^{-1}\sigma_i^{z}' \\ R_{31}^{-1}\sigma_i^{x}' + R_{32}^{-1}\sigma_i^{y}' + R_{33}^{-1}\sigma_i^{z}' \end{bmatrix}\right)^{z} \tag{5.6}$$

$$= h\left(R_{31}^{-1}\sigma_i^{x}' + R_{32}^{-1}\sigma_i^{y}' + R_{33}^{-1}\sigma_i^{z}'\right)$$

Hence, the final form of $H^{c'}$ is

$$H^{c'} = -J\sum_{ij}\bar{\sigma}_i'.\bar{\sigma}_j' - \sum_i h\left(R_{31}^{-1}\sigma_i^{x}' + R_{32}^{-1}\sigma_i^{y}' + R_{33}^{-1}\sigma_i^{z}'\right)$$

$$= -J\sum_{ij}\bar{\sigma}_i'.\bar{\sigma}_j' - \sum_i h_x'\sigma_i^{x}' + h_y'\sigma_i^{y}' + h_z'\sigma_i^{z}' = -J\sum_{ij}\bar{\sigma}_i'.\bar{\sigma}_j' - \sum_i \bar{h}'.\bar{\sigma}' \tag{5.7}$$

We here have defined effective magnetic field in S' to be $h_x' = hR_{31}^{-1}, h_y' = hR_{32}^{-1}, h_z' = hR_{33}^{-1}$

Retaining the assumption that the interaction is nearest neighbor, we obtain

$$H^{c'} = -J\sum_i \bar{\sigma}_i'.\bar{\sigma}_{i+1}' - \sum_i h\left(R_{31}^{-1}\sigma_i^x' + R_{32}^{-1}\sigma_i^y' + R_{33}^{-1}\sigma_i^z'\right)$$
$$= -J\sum_i \bar{\sigma}_i'.\bar{\sigma}_{i+1}' - \sum_i h_x'\sigma_i^x' + h_y'\sigma_i^y' + h_z'\sigma_i^z' = -J\sum_i \bar{\sigma}_i'.\bar{\sigma}_{i+1}' - \sum_i \bar{h}'.\bar{\sigma}' \tag{5.8}$$

This equation is to be used to evaluate dynamics of spins in central region. The Hamiltonian of spins of the lead does not change as we are now working in *S'*, the leads' coordinate system.

$$H^{L,R} = -J\sum_i \bar{\sigma}_i'.\bar{\sigma}_{i+1}' - \sum_i h_l\sigma_i^z' \tag{5.9}$$

From $H^{c'}$, we follow similar procedure as is used in deriving the dynamics of spin junction under uniform magnetic field to come up with the (surface) Green's function for the lead and the equation of motion of the spins in central region. There will be no change, as compared to the uniform field case, in the Green's function of the lead and such quantities as self energy and noise derived from the Green's function.

The Hamiltonian, in terms of a and $a^\dagger$ can be shown to be, upon getting rid of terms of second and higher orders,

$$H^{c}' = H_0^{c}' - \frac{1}{\sqrt{2}}\left(h_x' + ih_y'\right)a_i^\dagger' - \frac{1}{\sqrt{2}}\left(h_x' - ih_y'\right)a_i' \tag{5.10}$$

where H_0^{c}' is the usual spin wave Hamiltonian but with magnetic field h_z' in place of the usual variable. That is,

$$H_0^{c}' = \sum_{ij} H_{ij}^{c}'a_i^\dagger'a_j' = \sum_i -Ja_i^\dagger'a_{i+1}' + (2J + h_z')a_i^\dagger'a_i' - Ja_{i+1}^\dagger'a_i' \tag{5.11}$$

The equation of motion of the central region in terms of Bosonic annihilation and creation operators becomes, however, nontrivial and is given by

$$i\frac{da_i^{c}'}{dt} = -Ja_{i-1}' + (2J + h_z')a_i' - Ja_{i+1}' - \frac{1}{\sqrt{2}}\left(h_x' + ih_y'\right) \tag{5.12}$$

or

$$i\frac{da_i^{c\dagger}'}{dt} = Ja_{i-1}^\dagger' - (2J + h_z')a_i^\dagger' + Ja_{i+1}^\dagger' + \frac{1}{\sqrt{2}}\left(h_x' - ih_y'\right) \tag{5.13}$$

Following the same spirit as that used in Chapter 3 for uniform field case, we define three column vectors for annihilation operator a in the left lead, central and right lead in coordinate system S' and denote them by $a^L{}'$, $a^C{}'$ and $a^R{}'$. The equations of motion will then be used to study the dynamics of spins in junction as summarized by quantum Langevin equation,

$$i\frac{da^C{}'(t)}{dt} = H^C{}'a^C{}'(t) + \int_{t_0}^{t}\Sigma^{rL}{}'(t,t')a^C{}'(t')dt' + \int_{t_0}^{t}\Sigma^{rR}{}'(t,t')a^C{}'(t')dt' + \eta^L{}'(t) + \eta^R{}'(t) \tag{5.14}$$

or

$$i\frac{da^{c\dagger}{}'(t)}{dt} = -H^C{}'a^{c\dagger}{}'(t) - \int_{t_0}^{t}\Sigma^{rL}{}'(t',t)a^{c\dagger}{}'(t')dt' - \int_{t_0}^{t}\Sigma^{rR}{}'(t',t)a^{c\dagger}{}'(t')dt' - \eta^L{}'(t) - \eta^R{}'(t)\cdot \tag{5.15}$$

One important point is that now everything is expressed with respect to lead coordinate system S' where the variables originally expressed with respect to coordinate system S have been transformed to the corresponding variables in S'. The important changes are, first, in the form of equation of motion. Secondly, on coupling matrices V^{LC} and V^{RC} and this affects the friction and noise forces. These matrices are obtained by deriving the equations of motion of the spins in central region near the borders. Since the interaction is still nearest neighbor, however, the matrices are still expected to have only one nonzero element at the corner. The value of this non vanishing element is therefore equal to the coefficient of force term acting on the spin of central region nearest to border due to the spin of the lead nearest to the border. That is, from the equations of motion of the first and last spins of the central region,

$$i\frac{da_1{}'}{dt} = -Ja_0{}' + (2J + h_z{}')a_1{}' - Ja_2{}' - \frac{1}{\sqrt{2}}\left(h_x{}' + ih_y{}'\right) \tag{5.16}$$

$$i\frac{da_N{}'}{dt} = -Ja_{N-1}{}' + (2J + h_z{}')a_N{}' - Ja_{N+1}{}' - \frac{1}{\sqrt{2}}\left(h_x{}' + ih_y{}'\right) \tag{5.17}$$

We conclude that the coupling matrices between the central region and the leads are characterized by single matrix element $-J$ for both leads. This result is surprisingly

simple since we are dealing with different magnetic fields in different regions and thus expect to have the effect of magnetic field be reflected on the coupling matrices. This simplicity is however very natural because magnetic field is analogous to onsite potential and affects spin only individually and thus does not affect the exchange interaction between spins. The effect of the magnetic field (both its magnitude and different orientations and thus different orientations of the spins at ground state) are implicitly contained in the magnetic field components h_x, h_y and h_z that go directly into the Green's function and the quantum Langevin equation for the central region.

Derivation of Heat Flux from Local Energy Density

$$h_i = -Ja_i^{\dagger}{}'a_{i+1}' + (2J + h_z')a_i^{\dagger}{}'a_i' - Ja_{i+1}^{\dagger}{}'a_i' - \frac{1}{\sqrt{2}}(h_x' + ih_y')a_i^{\dagger}{}' - \frac{1}{\sqrt{2}}(h_x' - ih_y')a_i'$$

$$\frac{dh_i}{dt} = -J\frac{da_i^{\dagger}{}'}{dt}a_{i+1}' - Ja_i^{\dagger}{}'\frac{da_{i+1}'}{dt} + (2J + h_z')\frac{da_i^{\dagger}{}'}{dt}a_i' + (2J + h_z')a_i^{\dagger}{}'\frac{da_i'}{dt} - J\frac{da_{i+1}^{\dagger}{}'}{dt}a_i' - Ja_{i+1}^{\dagger}{}'\frac{da_i'}{dt}$$
$$- \frac{1}{\sqrt{2}}(h_x' + ih_y')\frac{da_i^{\dagger}{}'}{dt} - \frac{1}{\sqrt{2}}(h_x' - ih_y')\frac{da_i'}{dt} \qquad (5.18)$$

Using equations (5.12) and (5.13) for the time derivatives and continuity equation (3.37) it can be verified that

$$j_i' = -iJ^2a_i^{\dagger}{}'a_{i+2}' + iJ(2J + h_z')a_i^{\dagger}{}'a_{i+1}' - \frac{iJ}{\sqrt{2}}(h_x' + ih_y')a_i^{\dagger}{}' + \frac{iJ}{\sqrt{2}}(h_x' - ih_y')a_i' + iJ^2a_{i+2}^{\dagger}{}'a_i' - iJ(2J + h_z')a_{i+1}^{\dagger}{}'a_i'$$
$$j_i' = -iJ^2a_i^{\dagger}{}'a_{i+2}' + iJ^2a_{i+2}^{\dagger}{}'a_i' - iJ(2J + h_z')a_{i+1}^{\dagger}{}'a_i' + iJ(2J + h_z')a_i^{\dagger}{}'a_{i+1}' - \frac{iJ}{\sqrt{2}}(h_x' + ih_y')a_i^{\dagger}{}' + \frac{iJ}{\sqrt{2}}(h_x' - ih_y')a_i' \qquad (5.19)$$

In the limit when $\theta = 0, \phi = 0$,

$R_{31}^{-1} = 0, R_{32}^{-1} = 0, R_{33}^{-1} = 1.0$

So that $h_x' = h_y' = 0, h_z' = h$, then,

$$j_i' = -iJ^2a_i^{\dagger}{}'a_{i+2}' + iJ^2a_{i+2}^{\dagger}{}'a_i' - iJ(2J + h_z')a_{i+1}^{\dagger}{}'a_i' + iJ(2J + h_z')a_i^{\dagger}{}'a_{i+1}'$$

which is exactly the heat flux formula for uniform field case as can be seen by comparing this equation with equation (3.38). In other words,

$$j_i' = j_i - \frac{iJ}{\sqrt{2}}(h_x' + ih_y')a_i^{\dagger}{}' + \frac{iJ}{\sqrt{2}}(h_x' - ih_y')a_i' \qquad (5.20)$$

5.2.2 **Simulation Results on Magnetic Thermal Switch**

The lengthy analysis in previous section gives rise to several interesting features showing up in the simulations.

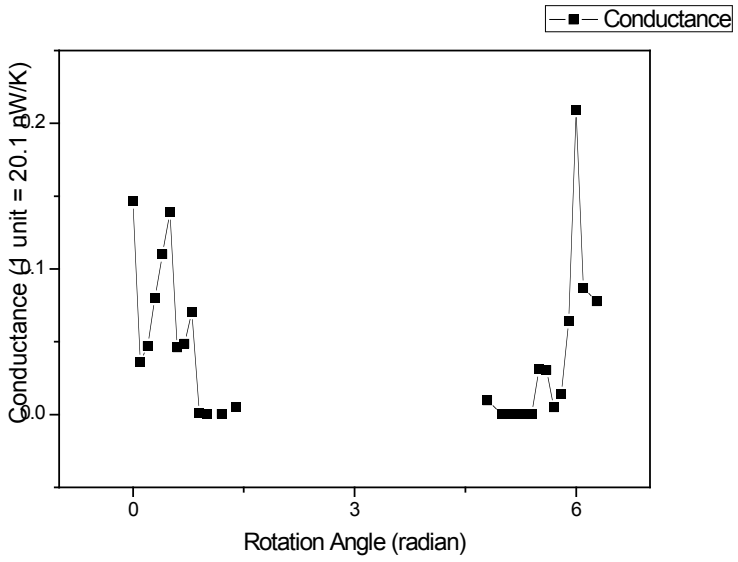

Fig. 5.3 Simulation result of thermal switch model performed at $T = 5{,}800K$ (transition region), $J = 1.4386 \times 10^{48} kg^{-1} m^{-2}$ (weak), $h = 1.0$, $N = 8$. Two cycles of 2^{20} MD steps are used with time step 0.01 and 2,000 steps for integration kernel. The rotation angle of magnetic field in the junction ranges from 0 to 2π radians. Only interval within $\pi/2$ radians about positive z axis (parallel direction) gives sensible conductance. Since spin wave approximation is used, the result is actually valid only for small range of angles about 0 and 2π. Nonlinear spin chain has to be used to obtain valid result at all ranges of rotation angle.

The simulations are performed at temperature *T = 4,640 K* which is in ballistic regime. The peak conductance on the right part of the figure is larger than the one on the left part on both figures. The simulation does show the decline of thermal conductance with increase in rotation angle. The system is periodic with full one cycle (360°) rotation but the pattern of decay is not simply a smooth decay as a simple educated guess may suggest. Beyond the bound of numerical error or fluctuation, the conductance shows sharp spikes and troughs along the curve. The overall pattern of the curve then looks quite similar to over damped oscillation. In other words, the curve consists of two periodic oscillations. One is oscillation with period of one full rotation (big oscillation)

and the small over damped oscillation with much smaller period. So, there are two main effects combining into one. First effect is decay of the conductance as the angle is increased. Secondly, the conductance oscillates with the increase in rotation angle. As the angle of rotation exceeds 90°, the simulation breaks down, conductance value either blows up to very large value or becomes not a number NaN . This indicates that the spin wave picture does not work if the twisting angle exceeds 90° because then the spin wave will be like flipped and this violates the ferromagnetic properties of the system because flipping of spin in classical picture means the spin system is anti-ferromagnetic.

With these properties, the model can be used as thermal switch over the range of rotation angle where the conductance oscillates with the angle from 0° to 90° both clock wise and anticlockwise. At angles larger than 90° in both directions, spin wave picture fails and the conductance effectively vanishes. This does not necessarily occurs if we do not assume spin wave approximation and use the fully nonlinear nature of spin system. Actually this simulation should be performed using nonlinear spin Hamiltonian but this linear version still can provide a good estimate of the former or otherwise much more complicated analysis has to be dealt with.

Unfortunately, for this particular model, the presence of odd product of operators makes it difficult for other methods to handle this problem. NEGF, for example, which relies on matrix formalism and is suitable for linear system will have to invoke higher excited states part of the full Hamiltonian matrix (the part other than the top left block in Fig. 2.2) in order to study this model. The size of matrix will then be $\left[\frac{1}{2}N(N+1)+1\right]^2$ compared to only $(N+1)^2$ when the Hamiltonian contains no such odd product of operators. This is one of the examples of problems that QMD can handle which many other methods will probably have hard time to deal with.

Conclusion

We have derived the same spin wave Hamiltonian matrix using classical spin dynamics, quantum mechanical operator formalism and second quantization method and this shows the consistency and equivalent interpretation of spin wave in different pictures or representations. This result forms the basis for linear study of thermal transport spin chain. We have derived the dispersion relation which is very crucial for explanation of various transport properties observed from simulation. With regard to simulation, to be precise, the dispersion relation determines the frequency range of excited spin waves contributing to the transmission of energy as reflected by Landauer formula as well as the frequency range of contributing modes of noise as reflected by noise spectrum.

We have used classical molecular dynamics with quasi classical approximation to study thermal transport in spin junction. The quasi classical approximation consists of using quantum Bose–Einstein heat bath instead of classical heat bath normally used in molecular dynamics and evaluating time evolution of operators rather than classical coordinate and momentum variables which are completely irrelevant for spin dynamics. The equation of motion is found to be first order in time derivative rather than second order. The Green's function does not have quadratic term in frequency and as a result, the noise spectrum is not an even function of frequency. It is shown using Nose-Hoover heat bath that classical heat bath cannot produce correct ballistic transport at low temperatures in nonlinear spin chain. Quantum annihilation and creation operators are the correct dynamical variables to be used in simulation of spin system. Quantum molecular dynamics is shown to be able to correctly reproduce the ballistic thermal transport in spin junction under spin wave approximation, in agreement with NEGF calculation. More importantly, when the fully nonlinear spin dynamics is used, the simulation is able to reconcile the quantum ballistic transport at low temperatures with the classical diffusive transport at high temperatures. From simulation results on various transport properties of spin chain which agree so well with experimental observations, consistent theoretical analyses are proposed to explain the observed phenomena.

Several theoretical conclusions have been inferred from simulation results. First,

spin chain under spin wave approximation yields ballistic transport with conductance increasing with temperature to a saturation value at very high temperatures but it decreases roughly linearly with magnetic field. This happens because by increasing temperature we excite more spin wave modes until we excite their all possible modes whereas increasing magnetic field we increase energy level spacing and thus excitation energy of spin wave. Putting in nonlinearity gives rise to intriguing temperature and magnetic dependences of thermal conductance of spin chain where the conductance increases with both parameters before asymptotically settling to the ballistic values. In the former, the low temperature behavior is clearly because linear and quantum effects dominate to give ballistic transport while at high temperatures non momentum-conserving spin wave scatterings take control to give classical diffusive transport. In the dependence on magnetic field, the initial increase in conductance is because magnetic field overcomes the nonlinear spin-spin exchange interaction to make transport more ballistic and in the very strong field limit, ballistic transport completely dominates that further increase in field strength means less spin wave modes excited.

Practical application of spin junction in thermal rectification is investigated. It is demonstrated rectifying effect does occur in simplest spin junction model which already incorporates asymmetric lead-junction coupling and nonlinear junction. The rectification turns out to be relatively strong relative to standard phonon or ideal two-level models. Other than rectification based on asymmetric coupling, rectification based on spectrum mismatch is also possible which according to dispersion relation, can be realized by applying magnetic field with different magnitudes to the two leads. The second application, the magnetic thermal switch in which we are free to rotate the field in the junction with respect to the fixed field in the leads, is particularly interesting because despite the use of spin wave approximation, the Hamiltonian involves the x and y components of Pauli spin matrices and so odd product of annihilation or creation operators in the second quantized form. There is allegedly non simple decay pattern of junction conductivity with the increase in deviation angle. There are definitely other models already proposed for such thermal switch which are most likely phonon-based. To the best of our knowledge, spin-based thermal switch as proposed here together with the accompanying analysis has never been studied before. With this study we hope that

there will be more interest in spin system and at the same time the use of our molecular dynamics formalism for broader applications in different scientific fields.

Bibliography

1. J.-S. Wang, Phys. Rev. Lett. 99, 160601 (2007)
2. J. T. Lü and J.-S. Wang, preprint arXiv: 0803.0368v2 (2008)
3. S. Lepri, R. Livi, and A. Politi, Phys. Rep. 377, 1 (2003)
4. S. Nose, J. Chem. Phys. 81, 511 (1984)
5. W. G. Hoover, Phys. Rev. A 31, 1695 (1985)
6. F. Heidrich-Meisner, A. Honecker, D.C. Cabra, and W. Brenig, Phys. Rev. B 68, 134436 (2003)
7. K. Saito, Phys. Rev. B 67, 064410 (2003)
8. A.L. Chernyshev and A.V. Roshkov, Phys. Rev. B 72, 104423 (2005)
9. A.L. Chernyshev, J. Magnetism and Magnetic Materials 310 (2007) 1263 - 1265
10. D.C. McCollum, R.L. Wild, and J. Callaway, Phys. Rev. 136, 2A (1964)
11. A.V. Savin, G.P. Tsironis, and X. Zotos, Phys. Rev. B 72, 140402(R) (2005)
12. K. Saito, Europhys. Lett., 61(1), pp. 34 – 40 (2003)
13. Y. Yan, C.-Q Wu, G. Casati, T. Prosen, and B. Li, Phys. Rev. B 77 , 172411 (2008)
14. J. L. Garcia-Palacios and F.J. Lazaro,Phys. Rev. B 58, 14937 (1998)
15. U. Nowak, R.W. Chantrell, and E.C. Kennedy, Phys. Rev. Lett. 84, 163 (2000)
16. R. L. Douglas, Phys. Rev. 129, 3 (1963)
17. C. Hess, C. Baumann, U. Ammerahl, B. Buchner, F. Heidrich-Meisner, W. Brenig, A. Revcolevschi, Phys. Rev. B 64, 184305 (2001)
18. A.V. Sologubenko, K. Gianno, H.R. Ott, U. Ammerahl, A. Revcolevschi, Phys. Rev. Lett. 84, A.V. Sologubenko, K. Gianno, H.R. Ott, A. Vietkine, A. Revcolevschi, Phys. Rev.B 64, 054412 (2001)
19. X. Zotos and P. Prelovsek, cond-mat/0304630 v2 (2003)
20. Y. I. Chang, G. C. Summerfield, and D. M. Kaplan, Phys. Rev. B 3, 9 (1971)
21. C. Kittel, Solid State Physics (8th Edition), John Wiley and Sons (2006)
22. J. Callaway, Quantum Theory of Solids Volume 1, Academic Press (1960)
23. T. Holstein and H. Primakoff, Phys. Rev. 58, 1098 (1940)
24. A. Dhar and D. Roy, J. Stat. Phys. 125, 801 (2006)

25. G. W. Ford, J. T. Lewis, and R. F. O'Connell, Phys. Rev. A 37, 11 (1987)
26. A.L.Fetter and Walecka, Quantum Theory of Many-Particle Systems, McGraw Hill Book Company (1971)
27. A. A. Abrikosov, L. P. Gorkov, and I. E. Dzyaloshinski, Quantum Field Theoretical Methods in Statistical Physics, Pergamon Press (1965)
28. H. Haug and A.-P. Jauho, Quantum Kinetics in Transport and Optics of Semiconductors, Springer (1996)
29. J.-S. Wang, J. Wang, and Nan Zeng, Phys. Rev. B 74, 033408 (2006); J.-S.Wang, Nan Zeng, J. Wang, and C-.K. Gan, Phys. Rev. E 75, 061128 (2007)
30. R. Landauer, IBM J. Res. Dev. 1, 223 (1957)
31. R. Landauer, Philos. Mag. 21, 863 (1970)
32. Terraneo, M. Peyrard, and G. Casati, Phys. Rev. Lett. 88, 9 (2002)
33. B. Li, Lei Wang, and Giulio Casati, Phys. Rev Lett. 93 (18):184301 (2004)
34. D. Segal and A. Nitzan, Phys. Rev. Lett. 94, 034301 (2005)
35. Z. Nan's PhD thesis (unpublished) (2008)
36. N. Yang, N. Li,L. Wang, and B. Li, Phys. Rev. B 76(2): 020301 (2007)

Appendix

Quantum Molecular Dynamics Code

```
/* This is a program to simulate spin-wave with quantum bath in 1D. The model is a standard Heisenberg spin-chain under spin-wave approximation. H = - Js sum sigma . sigma - hs sigma_z, where sigma is Pauli spin matrix.
  Internal units for computation:
  we set hbar = 1, k_B = 1, and choose
  energy - eV  (electron volt),  E0 = 1 eV
  time   - t0 = hbar/eV = 6.5822 x 10^(-16) sec
  k_B*temperature - eV, T0 = 1 eV/k_B = 11604 Kelvin
  conductance - lambda0 =(eV/t0/T0) = 1 eV k_B/hbar = 20.0976 nano-watts/Kelvin
  note the standard physical constants
  eV = 1.6022 x 10^(-19) joule
  k_B = 1.3807 x 10^(-23) joule/K
  amu = 1.6605 x 10^(-27) kg
  hbar = 1.0546 x 10^(-34) m^2kg/s
*/
#include  <stdio.h>
#include  <stdlib.h>
#include  <math.h>
#include  <assert.h>
#include  <time.h>

typedef double  real;                                   /* can change to long double, double, or float */

                                                        /* global variables are defined here */
                                                        /* model parameters */
const real Js = 1.0;                                    /* use const to prevent changes */
const real hs = 1.00;                                   /* reduced magnetic field */
const real S = 1.0;                                     /* spin value, should always be 1 */
real *xpastl, *ypastl, *xpastr, *ypastr;                /* x real, y imaginary */
real *selfleftx, *selflefty, *selfrightx, *selfrighty;  /* Sigma(t) */
```

```
real *etaleftx, *etalefty, *etarightx, *etarighty;              /* noises */
real leadFleftx, leadFrightx, leadFlefty, leadFrighty;
real h;                                                          /* MD step size = dt */
int length_kernel;                                               /* array size for integral term */
int ipt_now = 0, ipt_eta = 0;
void sfgreen(double w, double g[2]);
void selfenerg(real self_Re[], real self_Im[], int lenk);
void get_noise(real etax[], real etay[], int len, real T);
void flux(real*, real*,int);
void rungekutta(real*,real*,int);
void force(real*,real*,int,int);
real Heisenberg_Energy(real*, int);
double drand64(void);
void srand64(int seed);
real landauer(double T_L, double T_R);

int main(int argc, char **argv)
{
//  const real cof_eV_to_Kelvin = 11604.5;
//  const real cof_to_nW = 20.0976;
   const real cof_eV_to_Kelvin = 1.0;
  const real cof_to_nW = 1.0;                                    /* use internal units hbar=1, k_B=1 */
  real cof;
  real *z, *f, *J;
  real *pav,*Jav;
  real E0, E, Eav, E2av;
  real dE_low, dE_high;
  real jpass, jpass2, Jtot, norm;
  real T_begin, alpha;
  real T_low;                                                    /* temperature low end, i = 0 */
  real T_high;                                                   /* temperatures of heat bathes */
  int n, i, mdstep, cnt, MAX, MAX10, MAX_pass, pass;
  double r1, r2, Ti;
  int length_FFT;                          /* no need to be global, since it is used only in main */
```

```
  FILE *prompt_file, *in_file, *out_file, *lead_file;
  char *filename_Re_SE_w,*filename_Im_SE_w;
  char *filename_leftx,*filename_lefty,*filename_rightx,*filename_righty;                /* files for
sigma */
  char *filename_noise_left,*filename_noise_right;
  char *tmp_s;
  char *filename_dE;

  filename_dE = malloc(80*sizeof(char));
  assert(filename_dE != NULL);
  filename_dE = "dE.txt";
  filename_Re_SE_w = malloc(80*sizeof(char));
  assert(filename_Re_SE_w != NULL);
  filename_Im_SE_w = malloc(80*sizeof(char));
  assert(filename_Im_SE_w != NULL);
  filename_leftx = malloc(80*sizeof(char));
  assert(filename_leftx != NULL);
  filename_lefty = malloc(80*sizeof(char));
  assert(filename_lefty != NULL);
  filename_rightx = malloc(80*sizeof(char));
  assert(filename_rightx != NULL);
  filename_righty = malloc(80*sizeof(char));
  assert(filename_righty != NULL);
  filename_noise_left = malloc(80*sizeof(char));
  assert(filename_noise_left != NULL);
  filename_noise_right = malloc(80*sizeof(char));
  assert(filename_noise_right != NULL);
  tmp_s = malloc(101*sizeof(char));
  assert(tmp_s != NULL);
  n = 8;                                                    /* size in the middle part */
  h = 0.01;                                              /* h, a.k.a. dt, * length_kernel should
be about 10 */
                                                                /* main array sizes */
```

```
  length_kernel = 2000;                                   /*  length  for  calculating  int
sigm(t,t')a(t') dt' */
                                                        /* also the length to store *past* */
  length_FFT = pow(2.0, 22);                              /* for noises, must be a power of 2 */
  MAX = length_FFT -1;                                   /* minus 1 because we need next time in RK */
  T_begin = 0.500;
  alpha = 0.1;
  T_low = T_begin * (1.0 - alpha);
  T_high = T_begin * (1.0 + alpha);
  MAX_pass = 4;
  prompt_file = stdout;
  in_file = stdin;
  out_file = stdout;
  if(argc > 1)
  {       /* command line: a.out, or a.out in, or a.out in out */
   prompt_file = stderr;
   in_file = fopen(argv[1], "r");
   assert(in_file != NULL);
  }
  if(argc > 2)
  {
   out_file = fopen(argv[2], "w");
   assert(out_file != NULL);
  }
  filename_Re_SE_w = "Re_g_w.txt";
  filename_Im_SE_w = "Im_g_w.txt";
  filename_leftx = "gLx1_t.txt";
  filename_lefty = "gLy1_t.txt";
  filename_rightx = "gRx1_t.txt";
  filename_righty = "gRy1_t.txt";
  fprintf(prompt_file,"\n");
//  fclose(in_file);
  fprintf(out_file, "# dt = %g, N= %d, Js = %g, hs = %g (eV)\n",
                (double) h, n, (double) Js, (double) hs );
```

```
fprintf(out_file, "# sizeof(real)= %d, h = %g (6.58x10^(-16)sec)\n",(int) sizeof(real),(double) h);
fprintf(out_file, "MD steps MAX= %d,  MAX_pass= %d\n",MAX, MAX_pass);
fprintf(out_file, "# T_begin= %g (eV/k_B), alpha= %g\n",
                (double) T_begin, (double) alpha);
selfleftx = malloc(length_kernel*sizeof(real));
selflefty = malloc(length_kernel*sizeof(real));
selfrightx = malloc(length_kernel*sizeof(real));
selfrighty = malloc(length_kernel*sizeof(real));
assert(selfleftx != NULL);
assert(selflefty != NULL);
assert(selfrightx != NULL);
assert(selfrighty != NULL);
etaleftx = malloc(length_FFT*sizeof(real));
etalefty = malloc(length_FFT*sizeof(real));
etarightx = malloc(length_FFT*sizeof(real));
etarighty = malloc(length_FFT*sizeof(real));
assert(etaleftx != NULL);
assert(etalefty != NULL);
assert(etarightx != NULL);
assert(etarighty != NULL);
selfenerg(selfleftx, selflefty, length_kernel);
        /* left and right lead self-energy are the same for this model */
for(i = 0; i < length_kernel; ++i) {
  selfrightx[i] = selfleftx[i];
  selfrighty[i] = selflefty[i];
}
lead_file = fopen(filename_leftx, "w");
assert(lead_file != NULL);
for(i = 0; i < length_kernel; ++i)
{
fprintf(lead_file, "%lf\n", selfleftx[i]);
if(i == (length_kernel - 1))
          printf("left self energy x writing to file completed\n");
}
```

```
fclose(lead_file);
lead_file = fopen(filename_lefty, "w");
assert(lead_file != NULL);
for(i = 0; i < length_kernel; ++i)
{
fprintf(lead_file, "%lf\n", selflefty[i]);
if(i == (length_kernel - 1))
        printf("left self energy writing y to file completed\n");
}
fclose(lead_file);
lead_file = fopen(filename_rightx, "w");
assert(lead_file != NULL);
for(i = 0; i < length_kernel; ++i)
{
fprintf(lead_file, "%lf\n", selfrightx[i]);
if(i == (length_kernel - 1))
        printf("right self energy writing x to file completed\n");
}
fclose(lead_file);
lead_file = fopen(filename_righty, "w");
assert(lead_file != NULL);
for(i = 0; i < length_kernel; ++i)
{
fprintf(lead_file, "%lf\n", selfrighty[i]);
if(i == (length_kernel - 1))
        printf("right self energy writing y to file completed\n");
}
fclose(lead_file);
fprintf(out_file, "#\n# T (eV/k_B)   kappa_bar (eV k_B/hbar)    error\n");
fflush(out_file);
z = malloc(2*n*sizeof(real));
f = malloc(2*n*sizeof(real));
J = malloc(n*sizeof(real));    //current is real physical quantity, so it has no imaginary part, so only n degrees of freedom
```

```
Jav = malloc(n*sizeof(real));
pav = malloc(2*n*sizeof(real));
assert(z != NULL);
assert(f != NULL);
assert(J != NULL);
assert(Jav != NULL);
assert(pav != NULL);
xpastl = calloc(length_kernel, sizeof(real));
ypastl = calloc(length_kernel, sizeof(real));
xpastr = calloc(length_kernel, sizeof(real));
ypastr = calloc(length_kernel, sizeof(real));
assert(xpastl != NULL);
assert(ypastl != NULL);
assert(xpastr != NULL);
assert(ypastr != NULL);
srand48(time(NULL));
srand64(time(NULL));
for(i = 0; i <2*n ; ++i)
{
  r1 = drand48();
  r2 = drand64();
  Ti = T_low + i*(T_high-T_low)/(2*n);
  z[i] = 0.01*sqrt(Ti/Js)*(2.0*drand48()-1.0);
}
get_noise(etaleftx, etalefty, length_FFT, T_low);
get_noise(etarightx, etarighty, length_FFT, T_high);
ipt_eta = 0;                              /* pointer start from 0 */
for(mdstep = 1; mdstep < MAX ; ++mdstep)
{                                          /* equilibrate */
  rungekutta(z,f,n);
  if(mdstep == (MAX - 1))
    printf("equilibration process completed\n");
}
Eav = 0.0;
```

```
E2av = 0.0;
dE_low = 0.0;                /* energy pumped in/out of the center part */
dE_high = 0.0;
for(i = 0; i < n; ++i)
{
 pav[i] = 0.0;
 pav[i + n] = 0.0;
 Jav[i] = 0.0;
}
E0 = Heisenberg_Energy(z, n);
jpass = 0.0;                                /* sum j over pass */
jpass2 = 0.0;                               /* sum j^2 over pass */
MAX10 = MAX/10;
for(pass = 1; pass <= MAX_pass; ++pass)
{
                            /* each pass uses a new random noise */
 get_noise(etaleftx, etalefty, length_FFT, T_low);
 get_noise(etarightx, etarighty, length_FFT, T_high);
 ipt_eta = 0;
 Jtot = 0.0;
 for(mdstep = 0; mdstep < MAX10; ++mdstep) {
   rungekutta(z,f,n);          /* omit 10 percents for equilibration */
   assert(ipt_eta < length_FFT);    /* make sure noises are not run out */
   if(mdstep == (MAX10 - 1))
   printf("omitting 10 percents for equilibrium completed\n");
 }
 for(mdstep = MAX10; mdstep < MAX; ++mdstep) {
   rungekutta(z,f,n);
   assert(ipt_eta < length_FFT);
   E = Heisenberg_Energy(z, n);
   Eav += E;
   E2av += E*E;
   flux(z, J, n);
   for(i = 0; i < n; ++i) {
```

```
      pav[i] += f[i]*f[i];
      pav[i+n] += f[i+n]*f[i+n];
      Jav[i] += J[i];  //sum of current at each site over all the iterated MD steps
    }
    for(i = 1; i < n-2; ++i)
    {                                   /* skip the ends */
      Jtot += J[i];   //sum of current at all sites evaluated over all the iterated MD steps
    }
    dE_low += 2.0*( f[0]*leadFlefty - f[n]*leadFleftx );              //J[0]
    dE_high += 2.0*( f[n-1]*leadFrighty - f[2*n-1]*leadFrightx );   //J[n-1]
    lead_file = fopen(filename_dE, "w");
    assert(lead_file != NULL);
     fprintf(lead_file, "dE_high = %lf vs J[n-1] = %lf and dE_low = %lf vs J[0] = %lf\n",
dE_high,        dE_low, J[n-1], J[0]);
     fclose(lead_file);
    if(mdstep == (MAX - 1))
          printf("main iterations of MD completed\n");
  }
  cnt = n - 3;
  if(cnt > 0)
        {
    Jtot = Jtot/(MAX-MAX10)/cnt;
  }
  jpass += Jtot;         //one Jtot is calculated from one pass over all the iterated MD steps
  jpass2 += Jtot*Jtot;
 }                                      /* end pass */
 if(T_low != T_high)
 {
   cof = -cof_to_nW/(T_low-T_high);            /* internal units to nW/K */
 } else {
   cof = 1.0;
 }
 fprintf(out_file,   "%g          %g   ",      (double)   (cof_eV_to_Kelvin*T_begin),   (double)
(cof*jpass/MAX_pass));
```

```
if (MAX_pass > 1)
{
  fprintf(out_file, "  %g\n",  (double) (
    -cof*sqrt((jpass2/MAX_pass - (jpass/MAX_pass)*(jpass/MAX_pass))/(MAX_pass-1)) ) );
}
else
{
  fprintf(out_file, "\n");
}
fflush(out_file);
norm = (1.0/(MAX-MAX10))/ ((real) MAX_pass);
Eav *= norm;
E2av = (E2av*norm - Eav*Eav)/n/n;
if(E2av > 0.0)
{
  E2av = sqrt(E2av);
}
dE_low = dE_low*norm;
dE_high = dE_high*norm;
Jtot = 0.0;                    /* exclude baths and one more particle */
cnt = 0;
for(i = 1; i < n-2; ++i)
{
   Jtot += Jav[i];              // sum over all passes and all sites labelling the Jav[i]
   ++cnt;
}
if(cnt > 0)
{
   Jtot = Jtot*norm/cnt;
}
fprintf(out_file, "length_kernel = %d, T = %g      E=%g      <H>=%g      dH=%g
\n",length_kernel,(double) T_begin, (double) E,
              (double) (Eav/n), (double) E2av);
fprintf(out_file, "<j> = %g, dE(-)/dt= %g, dE(+)/dt= %g\n",
```

```
                (double) Jtot, (double) dE_low, (double) dE_high);
 fprintf(out_file, "kappa_J = %g, kappa_L= %g, kappa_R= %g\n",
       (double) (Jtot*cof), (double) (dE_low*cof), (double) (dE_high*cof) );
 fprintf(out_file,
       "spin no temperature (eV/k_B)  conductance I/(T_high-T_low)(eV k_B/hbar)\n");
 for(i = 0; i < n; ++i)
 {
  fprintf(out_file, "%5d     %10g   %10g\n", i,
        (double) (cof_eV_to_Kelvin*pav[i]*norm), (double) (cof*Jav[i]*norm) );
 }
 fprintf(out_file, "exact ballistic result= %g (eV k_B/hbar)\n",
       landauer(T_low, T_high) );
fclose(out_file);
 return 0;
}
void flux(real z[], real J[], int n)
{
  int i;
  for(i=0; i<n-2; i++)
  {
    J[i]  =  -(Js*S*(2*Js*S+hs)*(2*z[i]*z[i+1+n]-2*z[i+n]*z[i+1])+Js*Js*S*S*(2*z[i+n]*z[i+2]-
2*z[i]*z[i+2+n]));
  }
  J[n-2] = -(Js*S*(2*Js*S+hs)*(2*z[n-2]*z[2*n-1]-2*z[2*n-2]*z[n-1]));
  J[n-1] = 0.0;
}
/* Compute the derivative, including the frictional and noises, i.e., f = d a/dt = (-i/hbar)[ H a(t) +
int_0^\inf sigma(t') a(t-t') dt' + eta(t) ] see the definition for H below at sfgreen().  We have set
hbar = 1.
Separate real and imaginary part, we have da_R/dt = H a_I + F_I, da_I/dt = - H a_R - F_R.
F = int + noise. Since f, a, etc are complex, real part is stored at 0 to n-1, imaginary part n to 2n-1.
*/
void force(real* z,real* f, int n, int code)
{
```

```
  int i,j;
  real fricleftx, fricrightx, friclefty, fricrighty;
  real etaleftx_avg, etalefty_avg, etarightx_avg, etarighty_avg;

  f[0] = (2*Js*S+hs)*z[n] - Js*S*z[1+n];
  for(i=1;i<n-1;i++) {
    f[i] = (2*Js*S+hs)*z[i+n] - Js*S*z[i-1+n] - Js*S*z[i+1+n];
  }
  f[n-1] = (2*Js*S+hs)*z[2*n-1] - Js*S*z[2*n-2];
  f[n] = -(2*Js*S+hs)*z[0] + Js*S*z[1];
  for(i=n+1;i<2*n-1;i++) {
    f[i] = -(2*Js*S+hs)*z[i-n] + Js*S*z[i-1-n] + Js*S*z[i+1-n];
  }
  f[2*n-1] = -(2*Js*S+hs)*z[n-1] + Js*S*z[n-2];

  fricleftx = 0.0;
  fricrightx = 0.0;
  friclefty = 0.0;
  fricrighty = 0.0;
                                                                    /* -i int self[t'] a[t']
dt' */
  for(j = 0; j<length_kernel; j++) {
    i = (ipt_now-j+length_kernel)%(length_kernel);
    fricleftx += - selfleftx[j]*ypastl[i] - selflefty[j]*xpastl[i];
    friclefty += - selfleftx[j]*xpastl[i] + selflefty[j]*ypastl[i];
    fricrightx += - selfrightx[j]*ypastr[i] - selfrighty[j]*xpastr[i];
    fricrighty += - selfrightx[j]*xpastr[i] + selfrighty[j]*ypastr[i];
  }
  if(code == 1) {
    etaleftx_avg = etaleftx[ipt_eta];
    etalefty_avg = etalefty[ipt_eta];
    etarightx_avg = etarightx[ipt_eta];
    etarighty_avg = etarighty[ipt_eta];
  } else if(code == 2) {
```

```
    etaleftx_avg = 0.5*(etaleftx[ipt_eta + 1] + etaleftx[ipt_eta]);
    etalefty_avg = 0.5*(etalefty[ipt_eta + 1] + etalefty[ipt_eta]);
    etarightx_avg = 0.5*(etarightx[ipt_eta + 1] + etarightx[ipt_eta]);
    etarighty_avg = 0.5*(etarighty[ipt_eta + 1] + etarighty[ipt_eta]);
  } else if(code == 3) {
    etaleftx_avg = 0.5*(etaleftx[ipt_eta + 1] + etaleftx[ipt_eta]);
    etalefty_avg = 0.5*(etalefty[ipt_eta + 1] + etalefty[ipt_eta]);
    etarightx_avg = 0.5*(etarightx[ipt_eta + 1] + etarightx[ipt_eta]);
    etarighty_avg = 0.5*(etarighty[ipt_eta + 1] + etarighty[ipt_eta]);
  } else {
    assert (code == 4);
    etaleftx_avg = etaleftx[ipt_eta + 1];
    etalefty_avg = etalefty[ipt_eta + 1];
    etarightx_avg = etarightx[ipt_eta + 1];
    etarighty_avg = etarighty[ipt_eta + 1];
    ++ipt_eta;                                          /* ipt_eta incremented only here */
  }
  leadFleftx = fricleftx*h + etalefty_avg;
  leadFlefty = friclefty*h - etaleftx_avg;
  leadFrightx = fricrightx*h + etarighty_avg;
  leadFrighty = fricrighty*h - etarightx_avg;

  f[0] += leadFleftx;
  f[n-1] += leadFrightx;                                /* add random force eta */
  f[n] += leadFlefty;
  f[2*n-1] += leadFrighty;

  return;
}
/* standard 4th order Runge-Kutta, see, e.g., "Numerical Recipes",
  k1 = h f(t, z),  z = z(t),
  k2 = h f(t+h/2, z + (h/2)*k1),
  k3 = h f(t+h/2, z + (h/2)*k2),
  k4 = h f(t+h, z + h*k3),
```

```
  z(t+h) = z(t) + k1/6 + k2/3 + k3/3 + k4/6;
*/
void rungekutta(real z[],real f[],int n)
{
 real *rungekt1, *rungekt2, *rungekt3, *rungekt4; // each runge kutta function is of size n to handle n sites  together at one time
 real *zim;
 real hh;
 int code, i;

 rungekt1 = malloc(2*n*sizeof(real));
 rungekt2 = malloc(2*n*sizeof(real));
 rungekt3 = malloc(2*n*sizeof(real));
 rungekt4 = malloc(2*n*sizeof(real));
 assert(rungekt1 != NULL);
 assert(rungekt2 != NULL);
 assert(rungekt3 != NULL);
 assert(rungekt4 != NULL);
 zim = malloc(2*n*sizeof(real));
 assert(zim != NULL);
 hh = 0.5*h;
 for(i=0;i<2*n;i++)
 {
  zim[i] = z[i];
 }
 code = 1;
 force(z,f,n,code);
 for(i=0;i<2*n;i++)
 {
  rungekt1[i] = f[i];
  z[i] = zim[i] + hh*rungekt1[i];
 }
 code = 2;
 force(z,f,n,code);
```

```
 for(i=0;i<2*n;i++)
 {
   rungekt2[i] = f[i];
   z[i] = zim[i] + hh*rungekt2[i];
 }
 code = 3;
 force(z,f,n,code);
 for(i=0;i<2*n;i++)
 {
   rungekt3[i] = f[i];
   z[i] = zim[i] + h*rungekt3[i];
 }
 code = 4;
 force(z,f,n,code);
 for(i=0;i<2*n;i++)
 {
   rungekt4[i] = f[i];
 }
 for (i = 0; i<2*n; i++)
 {
  z[i] = zim[i] + (hh/3)*(rungekt1[i] + 2*rungekt2[i] + 2*rungekt3[i] + rungekt4[i]);
 }
 ipt_now = (ipt_now + 1) % length_kernel;
 xpastl[ipt_now] = z[0];                 /* ipt_now contains valid entry */
 xpastr[ipt_now] = z[n-1];
 ypastl[ipt_now] = z[n];                         /* force() need _past_ */
 ypastr[ipt_now] = z[2*n-1];

 free(rungekt1);
 free(rungekt2);
 free(rungekt3);
 free(rungekt4);
 free(zim);
}
```

```
#include <fftw3.h>
/* Generate noise based on spectra computed from surface Green's function.
   The noise spectrum function is
   F[w] = (f(w) + 1/2)hbar Gamma[w],  where f(w) = 1/(exp(w hbar/(k_B T))-1),
   Gamma = i(Sigma^r-Sigma^a) = -2 Im VgV.
   The variance of Fourier amplitude a or b is
   <a^2> = <b^2> = F[w]/(2*h*len).
   The length of noise is len, len = 2^n to be efficient for FFT.  The
   left and right lead differ only by the temperature T. */
void get_noise(real etax[], real etay[], int len, real T)
{
   fftw_complex *eta_w, *eta_t;
   fftw_plan p;
   real r1, r2, y, a, b, f, var;
   real w, dw, w_min, w_max, g[2];
   int i;

   const real delta = 0.0;              /* zero-point motion term, can be 0 */
   const real k_B = 1.0;
   const real hbar = 1.0;
   eta_w = (fftw_complex *) fftw_malloc(sizeof(fftw_complex) * len);
   eta_t = (fftw_complex *) fftw_malloc(sizeof(fftw_complex) * len);
   assert(eta_w != NULL);
   assert(eta_t != NULL);

   p = fftw_plan_dft_1d(len, eta_w, eta_t, FFTW_FORWARD, FFTW_ESTIMATE);
                                        /* model parameter Js and hs are global */
   w_min = hs;                                  /* region of the band, based on dispersion relation */
   w_max = 4*Js + hs;                   /* outside the band, g[1] = 0 */
   dw = 2.0*M_PI/(h*len);               /* h is global */

   for (i = 0; i < len; ++i) {
     if( i < len/2 ) {
```

```
      w = i*dw;
    } else {
      w = (i-len)*dw;
    }
    var = 0.0;                          /* outside the band, Im g = 0 */
    if(w >= w_min && w <= w_max) {
      sfgreen(w, g);
      f = delta + 1.0/(exp(hbar*w/(k_B*T)) - 1.0);
      var = -f*hbar*g[1]*Js*Js/(h*len);
    }
    assert(var >= 0.0);
    r1 = drand64();
    r2 = drand48();
    y = sqrt(-2.0*log(r1)*var);         /* box-muller for gaussian */
    a = y*cos(2*M_PI*r2);
    b = y*sin(2*M_PI*r2);
    eta_w[i][0] = a;
    eta_w[i][1] = b;
  }
  fftw_execute(p);
                                        /* integration factor taking care in var */
  for(i = 0; i < len; ++i) {
    etax[i] = eta_t[i][0];
    etay[i] = eta_t[i][1];
  }
  fftw_destroy_plan(p);
  fftw_free(eta_w);
  fftw_free(eta_t);
}
real Heisenberg_Energy(real z[], int n)
{
  int i;
  real Heisenergy;
  Heisenergy = 0.0;
```

```
  for(i=0; i<n-1;i++) {
    Heisenergy += -(2*Js*S + hs)*(z[i]*z[i]+z[i+n]*z[i+n])+2*Js*S*(z[i]*z[i+1]+z[i+n]*z[i+1+n]);
  }
  Heisenergy += - (2*Js*S + hs)*(z[n-1]*z[n-1]+z[2*n-1]*z[2*n-1]);
  return Heisenergy;
}
```

/* Compute the self-energy in time-domain according to Sigma(t) = Fourier transform of V g[w] V. Method: Let D = g^r - g^a = 2*I Im g^r. We then transform D[w] to D(t). Since g^a(t) = 0 for t > 0,

D(t) = g^r(t), for t > 0. We perform Fourier transform by simple integration -- this is more efficient and accurate than FFT. The function returns real and imaginary part of Sigma, of length lenk. We assume Vrc = Vlc = -Js. */

```
void selfenerg(real self_Re[], real self_Im[], int lenk)
{ real t, w, dw, g[2], factor;
  real w_min, w_max;
  int i;
  dw = 0.0010;                          /* spacings in omega, can be any small value */
  w_min = hs;                           /* region of the band, based on dispersion relation */
  w_max = 4*Js + hs;                        /* outside the band, g[1] = 0 */
  for(i = 0; i < lenk; ++i) {
    self_Re[i] = 0.0;
    self_Im[i] = 0.0;
    t = i*h;
    for(w = w_min; w <= w_max; w += dw) {
      sfgreen(w, g);
      self_Re[i] += g[1]*sin(w*t);
      self_Im[i] += g[1]*cos(w*t);
    }                       /* do int (g^r-g^a) exp(-iwt) dw/(2pi) */
  }
  factor = Js*Js*dw/M_PI;
  for(i = 0; i < lenk; ++i) {
    self_Re[i] *= factor;
    self_Im[i] *= factor;
```

```
  }
}
```

/* The surface Green's function is the g_{00} element of matrix equation (w + i eta - H) g = I, (eta > 0, for retarded version), where matrices are indexed from 0, 1, 2, ..., eta is a small quantity. H is the Hamiltonian of the lead with

$$H = \begin{bmatrix} 2Js+hs & -Js & 0 & 0 & \dots \\ -Js & 2Js+hs & -Js & 0 & \dots \\ 0 & -Js & 2Js+hs & -Js & 0 \\ 0 & 0 & 0 & -Js & \dots \\ \dots & & & . & \end{bmatrix}$$

For simplicity, and without loss of generality, we have set S = 1. The solution is g00 = -lambda/Js, where lambda is the solution of Js (1/lambda) + (w + i eta - 2Js - hs) + Js lambda = 0. We take the one with |lambda| < 1. It is given by lambda = - b +/- sqrt(b^2 - 1), where b = (w+i eta - 2Js - hs)/(2Js). The above Hamiltonian also implies that the dispersion relation for the spinwave is w = 2J(1-cos q) + h. Thus the magnon band is from h to h + 4Js. The function returns g[0] = Re g_00, g[1] = Im g_00. We use C99 features, some compiler may not work. But gcc will do.

*/

```
#include <complex.h>
void sfgreen(double w, double g[2])
{
  double complex b, lam, lam1, lam2, rt;
  double eta = 0.000001;

  b = (w + I*eta - 2.0*Js - hs)/(2.0*Js);
  rt = csqrt(b*b - 1.0);
  lam1 = - b + rt;
  lam2 = - b - rt;
  if(cabs(lam1) < 1.0) {
    lam = lam1;
  } else {
    lam = lam2;
  }
  lam = -lam/Js;
  g[0] = creal(lam);
```

```
  g[1] = cimag(lam);
  if(fabs(g[1]) < 1.0e-7) {              /* trim the small value to zero */
    g[1] = 0.0;
  }
  return;
}
static unsigned long long int xx = 1;
double drand64(void)
{
  xx = 6364136223846793005ll * xx + (long long int) 1;
  return (double) xx * 5.4210108624275218e-20;
}
void srand64(int seed)
{
  assert(sizeof(long long int) == 8);
  xx = seed;
}
/* Compute ballistic conductance according to Landauer formula. J = int hbar w T[w] (f_L - f_R)
dw/(2 Pi), T[w] = 1,  w_min < w < w_max, 0 otherwise. */
real landauer(double T_L, double T_R)
{
  real w, w_min, w_max, dw, f_L, f_R;
  real j;
  j = 0.0;
  w_min = hs;
  w_max = 4.0*Js + hs;
  dw = 0.001;
  for(w = w_min; w < w_max; w += dw) {
    f_L = 1.0/( exp(w/T_L) - 1.0);
    f_R = 1.0/( exp(w/T_R) - 1.0);
    j += w * (f_L - f_R);
  }
  j = dw*j/(T_L - T_R)/(2.0*M_PI);
  return j;
```

}